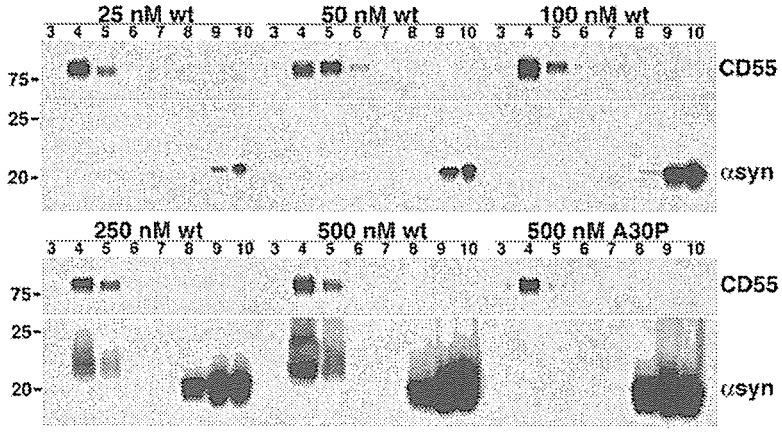

FIG. 1. **α-Synuclein binds to purified DRMs and the A30P mutation associated with PD disrupts the interaction.** Increasing concentrations of recombinant human α-synuclein (*wt*) (25–500 nM CBP fusion) were incubated at 30 °C for 30 min with DRMs purified from HeLa cells in the presence of bovine serum albumin (1%) as nonspecific competitor. Bound protein was separated from free by flotation on a sucrose density gradient, and the resulting fractions immunoblotted for α-synuclein. *Numbers above* the gels indicate fractions starting at the top of the gradient. Immunoblotting for the glycosylphosphatidylinositol-anchored protein CD55 identifies the rafts in fractions 4–6. Increasing amounts of α-synuclein result in increased binding, whereas the A30P mutant shows no binding even at the highest concentration tested (500 nM). DRM-bound α-synuclein also exhibits a shift in gel mobility similar to that previously observed (24). *Numbers* on the *left* indicate size markers (in kDa).

(data not shown), very similar to the results of other *in vitro* binding studies (20–23) but different from the lack of membrane association observed for the A30P mutant *in vivo* (17–19, 24). Supporting the possibility that A30P α-synuclein might interact nonspecifically with rafts under these conditions, we have observed substantial adsorption of α-synuclein to a variety of surfaces including plastic as well as membranes (data not shown). However, the high protein concentrations present in the cytoplasm of cells presumably reduce these nonspecific interactions *in vivo*. To test this possibility, we added BSA to the *in vitro* binding assay. Under these conditions, a substantial proportion of wild type α-synuclein (15% at 250 nM and ~25% at 500 nM) co-migrates in light fractions with CD55, a glycosylphosphatidylinositol-anchored protein of lipid rafts, indicating association with DRMs (Fig. 1). In contrast, A30P-α-synuclein does not bind to DRMs in the presence of BSA, even at the highest concentration of recombinant protein used in this study (Fig. 1). The association of wild type α-synuclein with DRMs is dose-dependent, with binding detectable in the mid-nanomolar range. We also found that varying the salt (NaCl or KCl), salt concentration (from 50 to 110 mM), or pH (from 6.5 to 8) has no detectable effect on the binding of α-synuclein to DRMs (data not shown). Because α-synuclein depends on lipid rafts for its specific localization to the nerve terminal, we examined binding to DRMs prepared from synaptic vesicles, and observed similar high affinity binding and sensitivity to the A30P mutation (data not shown). Because the recombinant protein used for these studies contains a 41-residue CBP fused to the N terminus of α-synuclein, we also removed the CBP tag by proteolytic cleavage with enterokinase (leaving no additional amino acids), and observed the same high affinity, specific binding to DRMs from HeLa cells and synaptic vesicles (data not shown). α-Synuclein bound to DRMs *in vitro* migrates more slowly by gel electrophoresis than soluble α-synuclein at the bottom of the flotation gradient (Fig. 1), indicating the acquisition *in vitro* of a raft-associated modification very similar to that observed *in vivo* (24). The *in vitro* binding assay therefore recapitulates many features observed for the interaction of α-synuclein with rafts in cells.

We used a competition assay to characterize further the association of α-synuclein with rafts. In particular, we assessed the ability of CBP-α-synuclein to compete with GST-α-synuclein for binding to DRMs. Fig. 2*A* shows that increasing amounts of wild type CBP-α-synuclein inhibit binding of 100 nM wild type GST-α-synuclein, indicating that the interaction with membranes is saturable. Quantification of multiple experiments reveals that concentrations of CBP-α-synuclein, ~0.5 μM, essentially eliminate binding of GST-α-synuclein (Fig. 2*B*), indicating an affinity that is at least in the mid-nanomolar range. Importantly, 2 μM A30P-CBP-α-synuclein fails to eliminate binding of wild type GST-α-synuclein (Fig. 2), confirming that this PD-associated mutant binds to DRMs with lower affinity than wild type (24).

Requirement for the Lipid Component of DRMs—To determine whether α-synuclein interacts with the protein or lipid component of rafts, we treated DRMs isolated from HeLa cells with proteinase K (PK) immobilized on agarose beads. After digestion for 5–60 min, PK-agarose was removed by sedimentation before adding recombinant α-synuclein. Strikingly, proteolytic digestion with PK did not reduce the interaction of α-synuclein with DRMs (Fig. 3*A*). However, a substantial proportion of CD55 remains intact even after prolonged incubation in proteinase K (Fig. 3*A*), raising questions about the extent of digestion. Resistance to proteolysis could simply reflect the presence of CD55 on the lumenal face of isolated DRMs, inaccessible to PK. Lumenal proteins presumably do not participate in the interaction with recombinant α-synuclein. We further confirmed that digestion in PK for 60 min largely eliminates DRM protein as detected by silver staining (Fig. 3*B*). In similar experiments using DRMs isolated from synaptic vesicles, treatment with PK also fails to inhibit binding of α-synuclein (data not shown). Remarkably, the α-synuclein bound to PK-digested DRMs still shows retarded electrophoretic mobility (Fig. 3*A*), indicating that this modification is unlikely to require proteins such as the raft-enriched kinases known to phosphorylate α-synuclein (32–34).

α-Synuclein Binds to Artificial Liposomes Resembling Lipid Rafts—To test further the hypothesis that α-synuclein associates with rafts through lipid rather than protein interactions, we prepared artificial membranes that resemble lipid rafts. Specifically, we used the "canonical" raft mixture composed of cholesterol, brain sphingomyelin (SM), and brain phospholipid (1:1:1 molar ratio), which mimics the enrichment of cholesterol and SM observed in native rafts (25). α-Synuclein binds to these liposomes and exhibits the same gel mobility shift observed when α-synuclein associates with native lipid rafts (Fig.

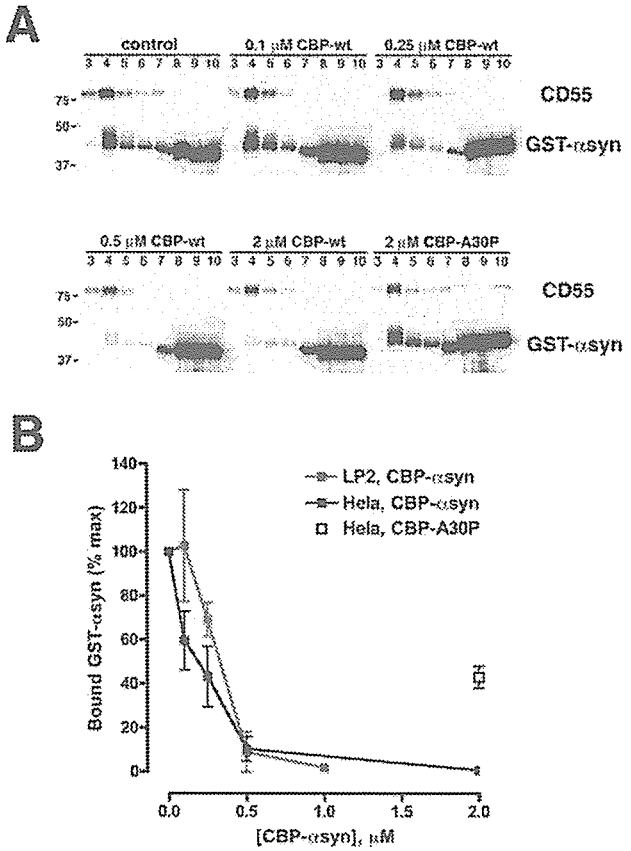

FIG. 2. **CBP-α-synuclein competes with GST-α-synuclein for binding to DRMs.** Wild type (*wt*) GST-α-synuclein (0.1 μM) and either wild type CBP-α-synuclein (0.1–2 μM) or CBP-A30P-α-synuclein (2 μM) were incubated with DRMs purified from HeLa cells or synaptic vesicles (LP2), and the raft-bound protein were separated by flotation through a sucrose density gradient as described in the legend to Fig. 1.*A*, fractions were immunoblotted for GST and in the case of HeLa DRMs, CD55. Increasing concentrations of wild type CBP-α-synuclein block the binding of wild type GST-α-synuclein to DRMs. In contrast, A30P CBP-α-synuclein reduces the binding of wild type protein only at high concentrations, confirming that the mutant has a lower affinity for DRMs than wild type α-synuclein. *Numbers* on the *left* indicate size markers (in kDa). *B*, the chemiluminescent output of Western blots was quantified by collecting the emitted light and the resulting signal normalized to the maximal signal obtained in the absence of competitor CBP fusion protein. The *graph* shows the mean of at least three independent experiments, and the *error bar* indicates S.D.

4*A*). Consistent with the results obtained from PK-digested DRMs, lipids alone thus support the binding of α-synuclein.

We varied the composition of the artificial membranes to identify the components of lipid rafts recognized by α-synuclein. Removal of cholesterol or SM (with replacement by brain PC) does not reduce the binding of α-synuclein to raft-like liposomes (Fig. 4*B*), indicating that the protein does not directly interact with these lipids. Indeed, a reduction in cholesterol content increases the binding of α-synuclein. The well described disruption of raft integrity by cholesterol depletion, rather than the loss of a direct interaction with α-synuclein, must therefore account for the effects of cholesterol depletion *in vivo* (24). In addition, it has been reported that the canonical raft mixture resides close to the miscibility transition temperature where small changes in vesicle composition have large effects on phase behavior (35, 36). The increased binding observed with decreased cholesterol may thus reflect an increase in the number of raft domains.

Acidic phospholipids promote the binding of α-synuclein to raft-like liposomes (Fig. 4*C*). PS is particularly effective, but phosphatidic acid also supports the interaction. In contrast, neutral phospholipids, such as PC and phosphatidylethanolamine, do not support the binding of α-synuclein to raft-like liposomes, consistent with previous reports using non-raft liposomes (20, 37). It is believed that lysines present on the α-helix induced by membrane association interact directly with the negatively charged phospholipid head group (20, 21, 23). However, other observations suggest that head group cannot be the only feature of raft phospholipid required for the membrane association of α-synuclein.

α-Synuclein Colocalizes with a Subset of Membrane PS—If PS confers the specific localization of α-synuclein to the synapse, then PS should exhibit a similar synaptic enrichment. To determine the distribution of PS, we have taken advantage of its specific recognition by annexin V (38). Most often used in live cells as a marker for the appearance of PS on the outer leaflet of the plasma membrane during apoptosis, annexin V has also been used in fixed cells to label intracellular compartments (39). Indeed, we observed extensive calcium-dependent labeling of primary hippocampal neurons with annexin V (Fig. 5*A*). To test further the specificity for PS, we adsorbed the annexin V with liposomes containing either PS and PC (1:1) or PC alone. Adsorption with membranes containing PS completely eliminated the labeling, whereas membranes containing PC alone had no effect, confirming the specificity of staining with annexin V. The extensive labeling of cultured neurons with annexin V thus reflects the true distribution of PS, which co-localizes only in part with the labeling for α-synuclein and the synaptic vesicle glutamate transporter VGLUT1 (Fig. 5*B*). Additional determinants must therefore account for the specific localization of α-synuclein to the nerve terminal.

Role of the Acyl Chain—α-Synuclein has been reported to bind monounsaturated free fatty acids such as oleic acid (18:1) and to form multimers in the presence of polyunsaturated fatty acids such as arachidonic acid (20:4) and docosahexaenoic acid (22:6) (40, 41). However, the role of phospholipid acyl chains in membrane binding of α-synuclein has not been addressed directly. We therefore varied the acyl chain composition of PS in liposomes containing cholesterol, sphingomyelin (SM), and PS (1:1:1). Because the brain PS used for these studies contains a mixture of acyl side chains (1.1% 16:0, 41.8% 18:0, 33.7% 18:1, 2.4% 20:4, 8.4% 22:6, 12.6% other), we first prepared membranes containing individual, defined synthetic forms of PS with both acyl chains identical (symmetric). However, none of the major components of brain PS (18:0, 18:1, 20:4, and 22:6) supports the interaction with α-synuclein when used alone (Fig. 6*A*). With large amounts of lipid and recombinant protein (8 times higher than the standard assay described above), we detected binding of α-synuclein to raft-like liposomes containing 18:1 PS alone (with cholesterol and SM) (Fig. 6*B*). Under these conditions, however, α-synuclein does not undergo the shift in gel mobility observed with rafts prepared from native tissue or with raft-like liposomes containing brain PS (Fig. 6*B*). We took advantage of this phenomenon to determine whether the altered mobility reflects a covalent modification. Analysis of trypsin-digested "shifted" α-synuclein (bound to membranes containing brain PS) and "unshifted" protein (bound to membranes with 18:1 PS) by mass spectrometry identified peptides spanning all of the α-synuclein sequence except the first 10 amino acids (MDVFMKGLSK) (data not shown). All peptides were detected only in an unmodified state, ruling out any stoichiometric covalent modifications of this part of the protein. Because we did not identify peptides spanning the first 10 residues of α-synuclein, we cannot exclude their potential modification. However, despite there being multiple studies dem-

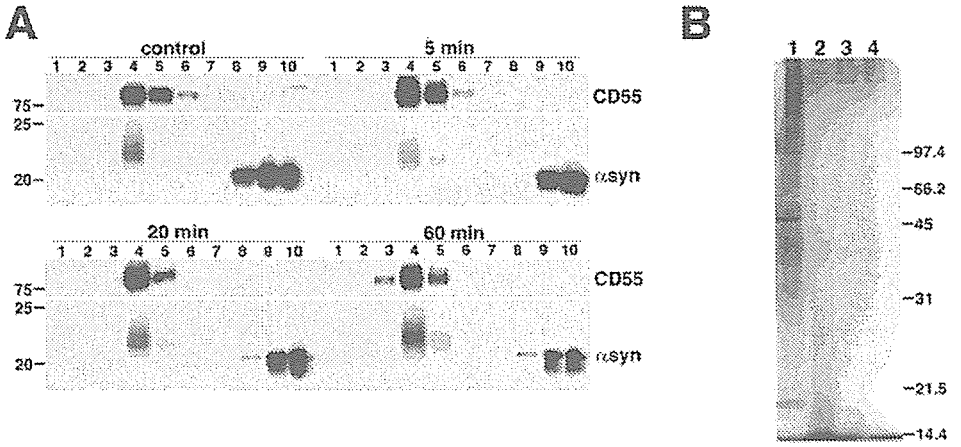

FIG. 3. **Binding of α-synuclein to DRMs does not require protein.** HeLa DRMs pretreated with PK for 5–60 min at 30 °C were incubated with recombinant human α-synuclein (50 nM CBP fusion) and subjected to flotation through a sucrose gradient as described above. Raft fractions are identified as CD55-positive. *A*, Western analysis of α-synuclein shows no effect of PK digestion on the raft association of α-synuclein. In addition, digestion with PK does not affect the shift in gel mobility of raft-bound α-synuclein. *B*, silver staining of raft extracts treated with PK for 0, 5, 20, and 60 min (*lanes 1–4*) shows a progressive loss of detectable raft protein. *Numbers* on the *left* indicate size markers (in kDa).

onstrating the post-translational modification of α-synuclein, none have reported modifications on any of the first 10 residues of the protein (32–34, 42–45). Together with the appearance of the gel mobility shift after binding to artificial membranes with no additional protein, the shift seems very unlikely to reflect a covalent modification.

Because no individual form of synthetic PS alone confers binding to α-synuclein, we combined PS with defined acyl chains in proportions mimicking those found in brain PS. Very similar to brain PS, this combination supports binding (Fig. 7*A*, *upper row*, *middle panel*). To determine the specific acyl chain requirements, we examined various mixtures of synthetic PS, focusing on simpler combinations with PS containing saturated or monounsaturated acyl chains and polyunsaturated side chains. To mimic the physiological proportions found in brain PS, we used more of the saturated or monounsaturated PS, and less of the polyunsaturated PS. Fig. 7*A* (*lower row*, *middle panel*) shows that 18:0 PS with either 20:4 or 22:6 PS exhibits weak binding. In contrast, 18:1 PS confers robust binding when combined with 20:4 or 22:6 PS (Fig. 7*A*, *lower row*, *left* and *right panels*), similar to that seen with brain PS and the reconstituted mixture of synthetic PS. α-Synuclein thus specifically requires both 18:1 PS and PS containing polyunsaturated acyl chains for its interaction with raft-like liposomes.

We further determined the proportion of 18:1 and 20:4 PS optimal for the interaction of α-synuclein with raft-like liposomes. Fig. 7*B* (*upper row*, *right panel*) shows that an equimolar combination of 18:1 and 20:4 PS (17% each) confers binding to raft-like liposomes. A 4-fold excess of 18:1 PS over 20:4 PS also promotes the binding of α-synuclein (Fig. 7*B*, *lower row*, *left panel*), but an excess of 20:4 PS over 18:1 PS (*upper row*, *middle panel*) does not. Further increases in the proportion of either 18:1 or 20:4 PS, with proportionate decreases of the other, completely abolish association of α-synuclein with the liposomes (Fig. 7*B*). Because 18:1 PS predominates over polyunsaturated PS in native membranes, α-synuclein apparently recognizes a physiologically relevant combination of fatty acid side chains.

Role of Phase Transition—Although lipid rafts have been shown to contain polyunsaturated fatty acids (46), they are generally thought to be enriched in long chain saturated acyl chains (47). The mechanism by which polyunsaturated phospholipid promotes the binding of α-synuclein to lipid rafts thus remains uncertain. α-Synuclein may interact with the PS containing polyunsaturated acyl chains inside raft domains. Alternatively, polyunsaturated acyl chains may promote a phase transition between raft and non-raft membranes. Indeed, the requirement of α-synuclein binding for both 18:1 and 20:4 PS supports a role for phase transition (Fig. 7). If phase transition is important for membrane association, the addition of any lipid that induces phase transition, including a lipid incapable by itself of binding α-synuclein, should support binding provided that at least some PS is present. We therefore supplemented the cholesterol/SM/18:1 PS liposomes, which cannot alone bind α-synuclein (Fig. 6*A*) with 20:4 PC, which also cannot by itself bind. The addition of 20:4 PC leads to a remarkable increase in the binding of α-synuclein (Fig. 8, *middle row*, *left panel*). Similarly, liposomes containing 18:1 PC and 20:4 PS, which fulfill both the head group and phase transition requirements, also support the binding of α-synuclein (Fig. 8, *middle row*, *middle panel*). However, membranes with the polyunsaturated acyl chain on the PS head group seem to bind with higher affinity than those with the monounsaturated acyl chain on PS within the context of brain PC (Fig. 8, *bottom row*). In addition to a requirement for phase transition, α-synuclein thus binds preferentially to PS containing polyunsaturated acyl chains.

DISCUSSION

To understand how the interaction with lipid rafts localizes α-synuclein to the nerve terminal, we have developed an *in vitro* assay for membrane binding by α-synuclein that recapitulates many features of the interaction observed *in vivo* (24). Using this assay, we show that α-synuclein binds saturably and with high affinity to DRMs isolated from HeLa cells or synaptic vesicles. The interaction is resistant to digestion of the rafts with proteinase K, suggesting a requirement for lipid and not protein. Confirming a direct interaction with lipid, α-synuclein binds to artificial liposomes that mimic rafts. Although other groups have previously shown that α-synuclein binds to liposomes *in vitro* (20–23), the assay described here differs in its sensitivity to the PD-associated mutation A30P. The A30P mutation disrupts the membrane interactions of α-synuclein in cells (17–19, 24), but has had little effect on binding to artificial membranes *in vitro* (20–23). Sensitivity to the A30P mutation thus supports the physiological relevance of this assay and of raft binding. The specificity of the assay presumably reflects the use of nonspecific competitor protein as

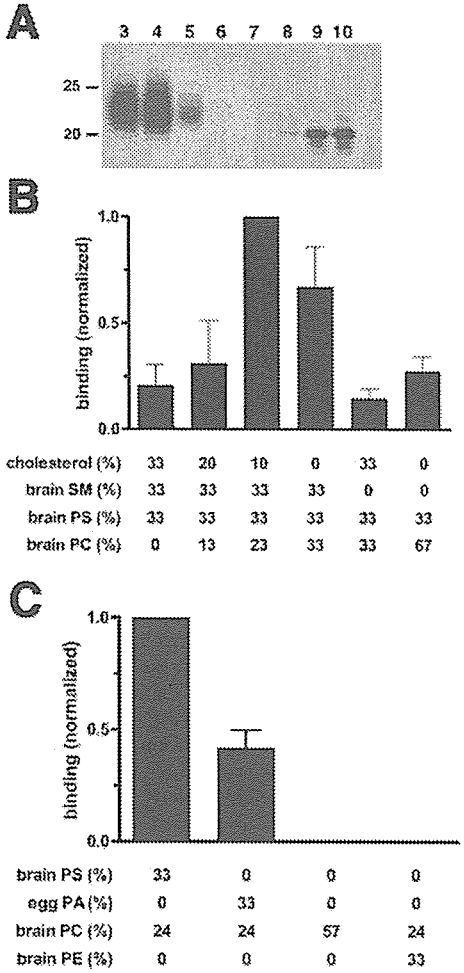

FIG. 4. **α-Synuclein binds to artificial membranes mimicking lipid rafts.** *A*, recombinant α-synuclein (100 nM CBP fusion) was incubated for 30 min at 30 °C with 25 μM artificial membranes containing cholesterol:brain sphingomyelin:brain PS (1:1:1 molar ratio), the bound protein was separated as described in the legend to Fig. 1, and the fractions immunoblotted for α-synuclein. α-Synuclein binds to these artificial membranes, and the bound protein exhibits a shift in gel mobility similar to that observed with rafts prepared from native tissue. *B*, the lipid composition of artificial membranes was modified by substituting cholesterol, brain SM, or brain PS with brain PC. After the binding assay and flotation gradient, the fractions were immunoblotted for human α-synuclein, the immunoreactivity was quantified and expressed as the ratio of bound (fractions 3–5) to unbound (fraction 9–10) α-synuclein, with normalization of the ratios to the maximal binding observed with cholesterol:SM:brain PS:brain PC (10:33:33:23). The results shown are the mean of three independent experiments ± S.D. *C*, α-synuclein (100 nM CBP fusion) was incubated with 25 μM artificial membranes prepared from 10% cholesterol, 33% brain SM, 24% brain PC, and various phospholipids. The binding assay, flotation gradient, and Western analysis were performed as in *A*. α-Synuclein binds only to lipids containing either the acidic PS or phosphatidic acid (*PA*), but not the neutral PC or phosphatidylethanolamine (*PE*). Data shown are the mean of three experiments ± S.D.

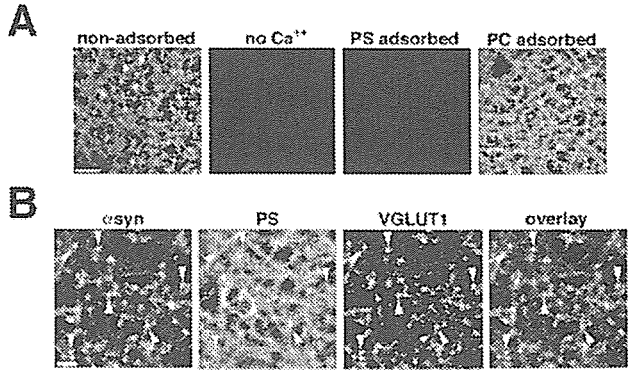

FIG. 5. **α-Synuclein co-localizes with a small subset of neuronal PS.** *A*, fixed hippocampal neurons were stained for PS using annexin V-Alexa 647 (non-adsorbed). The annexin V conjugate binds to all neuronal processes without enrichment in any particular compartment. Removal of calcium (no Ca^{2+}) and adsorption with liposomes containing PC:PS (1:1; PS adsorbed) but not PC alone (PC adsorbed) abolishes labeling with annexin V, confirming the specificity for PS. *Size bar*, 10 μm. *B*, α-synuclein co-localizes with only a subset of PS at synaptic sites that also label for synaptic vesicle glutamate transporter VGLUT1. α-Synuclein thus requires more than the PS head group for localization to the nerve terminal. *Arrowheads* point to synapses labeling for α-synuclein (*green* in merged image), PS (*blue* in merged image), and VGLUT1 (*red* in merged image). *Size bar*, 2 μm.

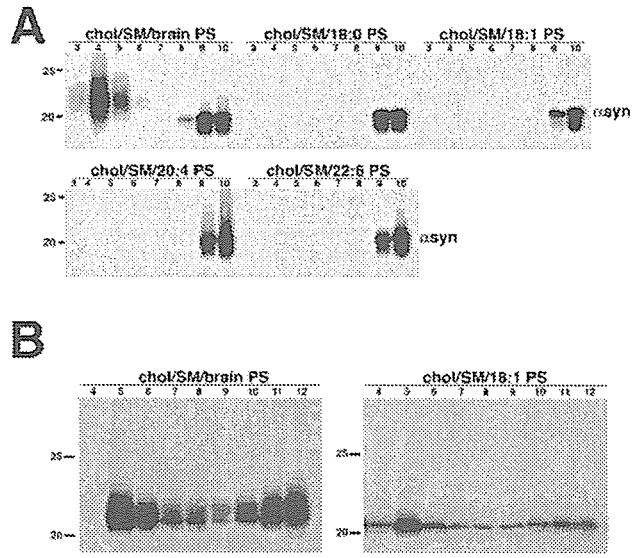

FIG. 6. **α-Synuclein does not bind to raft-like artificial membranes containing synthetic PS with a single defined fatty acyl chain.** *A*, α-synuclein (100 nM CBP fusion) was incubated with 25 μM artificial membranes containing equimolar ratios of cholesterol (*chol*), brain SM, and the indicated brain or synthetic PS. Binding, separation, and Western analysis were performed as described in previous figures. α-Synuclein (*α-syn*) binds strongly only to liposomes containing brain PS. *B*, α-synuclein interacts with raft-like liposomes containing 18:1 PS when protein and lipid are present at higher concentrations (here 8 μM α-synuclein and 1 mM lipid). Under these conditions, the gel mobility of α-synuclein (including soluble protein at the bottom of the gradient as well as membrane-bound protein in higher fractions) is retarded when interacting with brain PS (*left*), but not when interacting with 18:1 PS (*right*). *Numbers* on the *left* indicate size markers (kDa).

well as the raft-like nature of the membranes.

We previously observed that the α-synuclein associated with lipid rafts exhibits a shift in gel mobility (24). α-Synuclein indeed undergoes a conformational change from unstructured to α helical on binding to a variety of membranes *in vitro* (20, 23, 37, 48). However, other studies do not report an alteration in electrophoretic mobility of α-synuclein upon membrane binding. In general, these studies have used artificial membranes containing only synthetic phospholipid, suggesting that native membranes contain an activity missing from artificial membranes, which is required for the modification. The phosphorylation of α-synuclein by tyrosine kinases associated with lipid rafts raised the possibility that the observed gel shift reflects a post-translational modification (32–34, 44). However, extensive proteolysis of purified lipid rafts with proteinase K does not reduce either the binding or gel shift of α-synuclein.

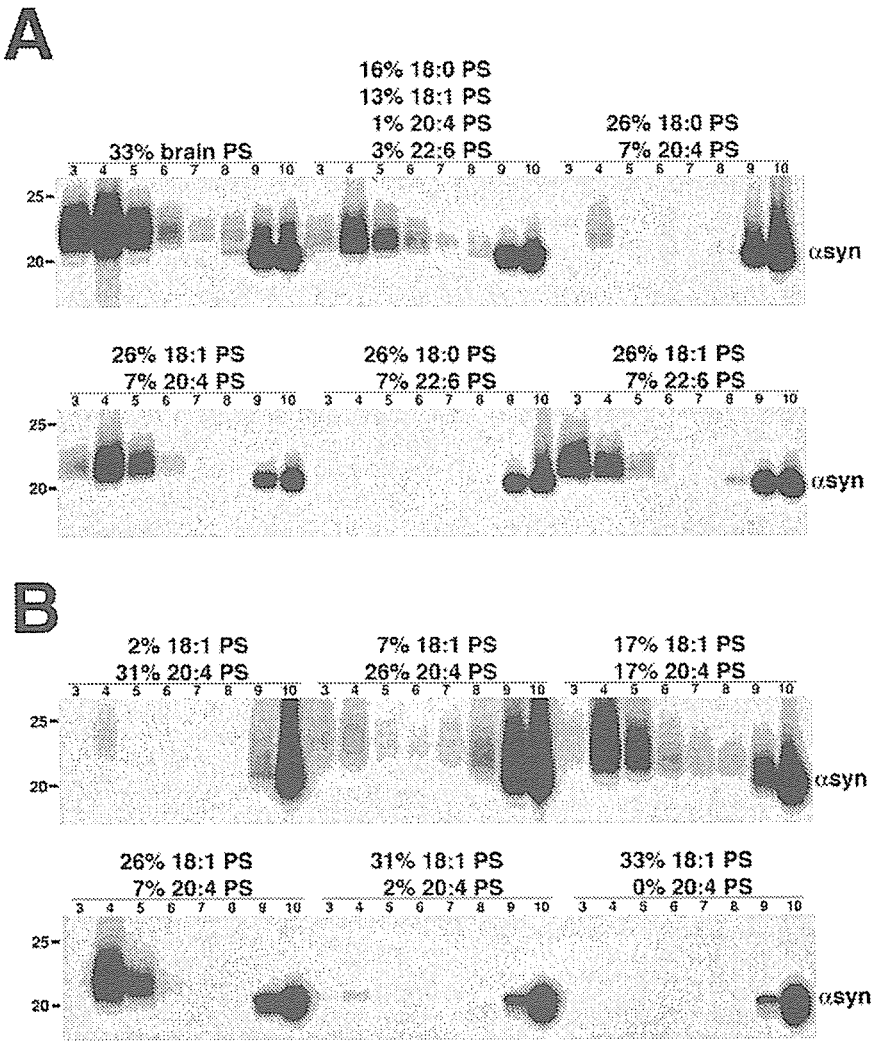

FIG. 7. **α-Synuclein binding requires PS with both mono- and polyunsaturated fatty acyl chains.** *A*, α-synuclein (*α-syn*) (100 nM CBP fusion) was incubated with liposomes containing equimolar concentrations of cholesterol, brain SM, and the indicated PS. Brain PS and a mixture that mimics brain PS (16% 18:0, 13% 18:1, 1% 20:4, 3% 22:6 PS) support the binding of α-synuclein. The minimal requirement for membrane association is 18:1 PS in the presence of a polyunsaturated PS (either 20:4 or 22:6). 18:0 PS cannot substitute for 18:1 PS. *B*, binding of α-synuclein to raft-like membranes containing different ratios of 18:1 and 20:4 PS shows that although equimolar concentrations of 18:1 and 20:4 PS (17% each) support membrane association, a larger proportion of 18:1 than 20:4 PS confers more binding than a larger proportion of 20:4 PS. *Numbers* on the *left* indicate size markers (kDa).

The altered gel mobility also persists when using artificial membranes that mimic lipid rafts, confirming that no additional protein is required for the modification or for binding. Interestingly, one previous report has shown a similar shift in the electrophoretic mobility of α-synuclein when using native brain rather than synthetic phospholipid (40). Mass spectrometry analysis of gel-shifted α-synuclein now reveals only unmodified peptides covering >90% of the α-synuclein sequence, which are identical to peptides derived from the unshifted protein. Taken together, these observations strongly suggest that the shift in gel mobility reflects a conformational change rather than a covalent modification. Raft-like membranes containing anionic brain phospholipid thus reproduce features of the interaction with native lipids not previously observed with synthetic liposomes.

What confers the specific binding and modification of α-synuclein by raft-like membranes? Cholesterol does not appear required. In fact, α-synuclein binds more strongly to membranes containing low or no cholesterol than the 33% classically used to produce raft-like membranes. The ability of cholesterol depletion to eliminate the raft association and synaptic localization of α-synuclein thus reflects the dependence of raft integrity on cholesterol, not a direct interaction of cholesterol with α-synuclein. Although it promotes binding to α-synuclein in the absence of cholesterol, sphingolipid also does not appear crucial for the interaction. Similar to previous reports, we find that α-synuclein binding requires acidic phospholipid, in particular PS. However, individual synthetic forms of PS do not support binding. Rather, we find that a very specific combination of 18:1 PS and PS with polyunsaturated acyl chains is required both to bind and shift the electrophoretic mobility of α-synuclein. Supporting the physiological relevance of this combination, ratios reflecting the preponderance of 18:1 over polyunsaturated acyl chains in native membranes are optimal for binding to α-synuclein. Furthermore, the addition of 18:1 PC to 20:4 PS confers binding to

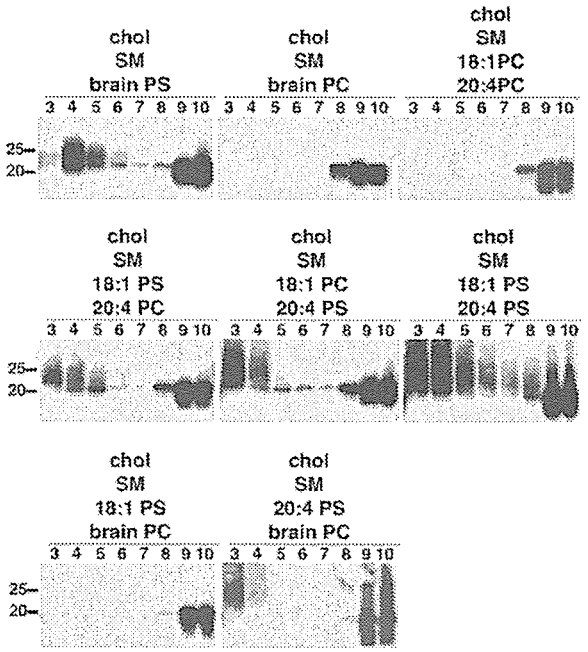

FIG. 8. **Phase transition is required for the binding of α-synuclein to raft-like liposomes.** *Top row*, α-synuclein (100 nM CBP fusion) was incubated with liposomes containing an equimolar mixture of cholesterol (*chol*), brain SM, and the indicated phospholipids, and analyzed as described above. Brain PS but not brain PC or synthetic PC (1:1 ratio of 18:1 and 20:4 PC) support the binding of α-synuclein. *Middle row*, the addition of either 20:4 PC (*left*) or 18:1 PC (*middle*) to 18:1 or 20:4 PS confers binding to α-synuclein. Because the PC head group alone does not support binding, the synthetic forms of PC presumably act by promoting a phase transition between monounsaturated and polyunsaturated fatty acyl chains. *Bottom row*, when added to brain PC, 20:4 PS confers substantially more binding to α-synuclein than 18:1 PS, suggesting specific recognition of the PS head group in the context of polyunsaturated fatty acyl chains. *Numbers* on the *left* indicate size markers (kDa).

α-synuclein even though PC cannot by itself support binding. Conversely, the addition of 20:4 PC to 18:1 PS also promotes binding. The requirement for both mono- and polyunsaturated acyl chains strongly suggests that the interaction of α-synuclein requires membrane with two distinct phases. The requirement for a phase transition may indeed account for the specific association of α-synuclein with rafts, which are considered a liquid-ordered phase distinct from the rest of the liquid-disordered cell membrane (47). Again, previous work has not shown such stringent requirements for the membrane association of α-synuclein, presumably because the specificity observed here depends on the high concentration of nonspecific competitor protein that mimic physiologic conditions in the cytoplasm.

In addition to the requirement for acidic head group and phase transition, we find that α-synuclein binds more strongly to membrane when the polyunsaturated acyl chain of the phospholipid resides on the PS head group. This remarkable specificity presumably reflects an interaction of α-synuclein with both acyl chain and head group. Consistent with the specificity for a particular combination of PS, α-synuclein colocalizes with only a small subset of the PS labeled by annexin V in neurons. Interestingly, the analysis of α-synuclein knock-out mice has shown increases in the level of polyunsaturated fatty acids (49), but the relationship of these changes to the membrane association of α-synuclein remains unclear. In addition, α-synuclein has been reported to bind free oleic acid *in vitro* (50) and to multimerize in the presence of polyunsaturated fatty acids (40), but a specific role for these acyl chains in the membrane association of α-synuclein has not been appreciated before. α-Synuclein has also been reported to bind lipid droplets produced by treatment of cells with oleic acid (18). However, it has remained unclear whether oleic acid simply induces lipid droplets to which α-synuclein can bind. Our results suggest the alternative explanation that α-synuclein interacts directly with the oleoyl side chain of phospholipid in the droplets.

In conclusion, we find that the membrane association of α-synuclein depends on the recognition of phospholipid head group and acyl chain, including phase transition and specific side chain composition. The assay we used to identify these requirements was designed to reproduce the interaction between α-synuclein and native membranes. Thus, the combination of membrane properties identified using this assay presumably contributes to the specific presynaptic localization of α-synuclein. To understand the normal function of this protein as well as its role in PD, future work will need to evaluate the membrane association of α-synuclein in the physiological context of the nerve terminal.

REFERENCES

1. Polymeropoulos, M. H., Lavedan, C., Leroy, E., Ide, S. E., Dehejia, A., Dutra, A., Pike, B., Root, H., Rubenstein, J., Boyer, R., Stenroos, E. S., Chandrasekharappa, S., Athanassiadou, A., Papapetropoulos, T., Johnson, W. G., Lazzarini, A. M., Duvoisin, R. C., Di Iorio, G., Golbe, L. I., and Nussbaum, R. L. (1997) *Science* **276**, 2045–2047
2. Kruger, R., Kuhn, W., Muller, T., Woitalla, D., Graeber, M., Kosel, S., Przuntek, H., Epplen, J. T., Schols, L., and Riess, O. (1998) *Nat. Genet.* **18**, 106–108
3. Zarranz, J. J., Alegre, J., Gomez-Esteban, J. C., Lezcano, E., Ros, R., Ampuero, I., Vidal, L., Hoenicka, J., Rodriguez, O., Atares, B., Llorens, V., Gomez Tortosa, E., del Ser, T., Munoz, D. G., and de Yebenes, J. G. (2004) *Ann. Neurol.* **55**, 164–173
4. Singleton, A. B., Farrer, M., Johnson, J., Singleton, A., Hague, S., Kachergus, J., Hulihan, M., Peuralinna, T., Dutra, A., Nussbaum, R., Lincoln, S., Crawley, A., Hanson, M., Maraganore, D., Adler, C., Cookson, M. R., Muenter, M., Baptista, M., Miller, D., Blancato, J., Hardy, J., and Gwinn-Hardy, K. (2003) *Science* **302**, 841
5. Spillantini, M. G., Crowther, R. A., Jakes, R., Hasegawa, M., and Goedert, M. (1998) *Proc. Natl. Acad. Sci. U. S. A.* **95**, 6469–6473
6. Spillantini, M. G., Crowther, R. A., Jakes, R., Cairns, N. J., Lantos, P. L., and Goedert, M. (1998) *Neurosci. Lett.* **251**, 205–208
7. Galvin, J. E., Uryu, K., Lee, V. M., and Trojanowski, J. Q. (1999) *Proc. Natl. Acad. Sci. U. S. A.* **96**, 13450–13455
8. Maroteaux, L., Campanelli, J. T., and Scheller, R. H. (1988) *J. Neurosci.* **8**, 2804–2815
9. Withers, G. S., George, J. M., Banker, G. A., and Clayton, D. F. (1997) *Dev. Brain Res.* **99**, 87–94
10. Murphy, D. D., Rueter, S. M., Trojanowski, J. Q., and Lee, V. M. (2000) *J. Neurosci.* **20**, 3214–3220
11. Abeliovich, A., Schmitz, Y., Farinas, I., Choi-Lundberg, D., Ho, W. H., Castillo, P. E., Shinsky, N., Verdugo, J. M., Armanini, M., Ryan, A., Hynes, M., Phillips, H., Sulzer, D., and Rosenthal, A. (2000) *Neuron* **25**, 239–252
12. Cabin, D. E., Shimazu, K., Murphy, D., Cole, N. B., Gottschalk, W., McIlwain, K. L., Orrison, B., Chen, A., Ellis, C. E., Paylor, R., Lu, B., and Nussbaum, R. L. (2002) *J. Neurosci.* **22**, 8797–8807
13. Ueda, K., Fukushima, H., Masliah, E., Xia, Y., Iwai, A., Yoshimoto, M., Otero, D. A., Kondo, J., Ihara, Y., and Saitoh, T. (1993) *Proc. Natl. Acad. Sci. U. S. A.* **90**, 11282–11286
14. George, J. M., Jin, H., Woods, W. S., and Clayton, D. F. (1995) *Neuron* **15**, 361–372
15. Iwai, A., Masliah, E., Yoshimoto, M., Ge, N., Flanagan, L., de Silva, H. A., Kittel, A., and Saitoh, T. (1995) *Neuron* **14**, 467–475
16. Kahle, P. J., Neumann, M., Ozmen, L., Muller, V., Jacobsen, H., Schindzielorz, A., Okochi, M., Leimer, U., van Der Putten, H., Probst, A., Kremmer, E., Kretzschmar, H. A., and Haass, C. (2000) *J. Neurosci.* **20**, 6365–6373
17. Jensen, P. H., Nielsen, M. S., Jakes, R., Dotti, C. G., and Goedert, M. (1998) *J. Biol. Chem.* **273**, 26292–26294
18. Cole, N. B., Murphy, D. D., Grider, T., Rueter, S., Brasaemle, D., and Nussbaum, R. L. (2002) *J. Biol. Chem.* **277**, 6344–6352
19. Outeiro, T. F., and Lindquist, S. (2003) *Science* **302**, 1772–1775
20. Davidson, W. S., Jonas, A., Clayton, D. F., and George, J. M. (1998) *J. Biol. Chem.* **273**, 9443–9449
21. Eliezer, D., Kutluay, E., Bussell, R., Jr., and Browne, G. (2001) *J. Mol. Biol.* **307**, 1061–1073
22. Jo, E., Fuller, N., Rand, R. P., St. George-Hyslop, P., and Fraser, P. E. (2002) *J. Mol. Biol.* **315**, 799–807
23. Chandra, S., Chen, X., Rizo, J., Jahn, R., and Sudhof, T. C. (2003) *J. Biol. Chem.* **278**, 15313–15318
24. Fortin, D. L., Troyer, M. D., Nakamura, K., Kubo, S., Anthony, M. D., and Edwards, R. H. (2004) *J. Neurosci.* **24**, 6715–6723
25. Ediding, M. (2003) *Annu. Rev. Biophys. Biomol. Struct.* **32**, 257–283
26. Jo, E., McLaurin, J., Yip, C. M., St. George-Hyslop, P., and Fraser, P. E. (2000) *J. Biol. Chem.* **275**, 34328–34334

27. Narayanan, V., and Scarlata, S. (2001) *Biochemistry* **40**, 9927–9934
28. Higgins, D., and Banker, G. A. (1998) in *Culturing Nerve Cells* (Banker, G. A., and Goslin, K., eds) 2nd Ed., pp. 37–78, MIT Press, Cambridge, MA
29. Huttner, W. B., Schiebler, W., Greengard, P., and De Camilli, P. (1983) *J. Cell Biol.* **96**, 1374–1388
30. Hell, J. W., and Jahn, R. (1994) in *Cell Biology, A Laboratory Handbook* (Celis, J. E., ed) Vol. 1, pp. 567–574, Academic Press, San Diego, CA
31. Field, K. A., Holowka, D., and Baird, B. (1995) *Proc. Natl. Acad. Sci. U. S. A.* **92**, 9201–9205
32. Pronin, A. N., Morris, A. J., Surguchov, A., and Benovic, J. L. (2000) *J. Biol. Chem.* **275**, 26515–26522
33. Nakamura, T., Yamashita, H., Nagano, Y., Takahashi, T., Avraham, S., Avraham, H., Matsumoto, M., and Nakamura, S. (2002) *FEBS Lett.* **521**, 190–194
34. Ellis, C. E., Schwartzberg, P. L., Grider, T. L., Fink, D. W., and Nussbaum, R. L. (2001) *J. Biol. Chem.* **276**, 3879–3884
35. Veatch, S. L., and Keller, S. L. (2003) *Biophys. J.* **84**, 725–726
36. Veatch, S. L., and Keller, S. L. (2003) *Biophys. J.* **85**, 3074–3083
37. Perrin, R. J., Woods, W. S., Clayton, D. F., and George, J. M. (2000) *J. Biol. Chem.* **275**, 34393–34398
38. Gerke, V., and Moss, S. E. (2002) *Physiol. Rev.* **82**, 331–371
39. Hirono, M., Denis, C. S., Richardson, G. P., and Gillespie, P. G. (2004) *Neuron* **44**, 309–320
40. Perrin, R. J., Woods, W. S., Clayton, D. F., and George, J. M. (2001) *J. Biol. Chem.* **276**, 41958–41962
41. Sharon, R., Bar-Joseph, I., Frosch, M. P., Walsh, D. M., Hamilton, J. A., and Selkoe, D. J. (2003) *Neuron* **37**, 583–595
42. Okochi, M., Walter, J., Koyama, A., Nakajo, S., Baba, M., Iwatsubo, T., Meijer, L., Kahle, P. J., and Haass, C. (2000) *J. Biol. Chem.* **275**, 390–397
43. Shimura, H., Schlossmacher, M. G., Hattori, N., Frosch, M. P., Trockenbacher, A., Schneider, R., Mizuno, Y., Kosik, K. S., and Selkoe, D. J. (2001) *Science* **293**, 263–269
44. Nakamura, T., Yamashita, H., Takahashi, T., and Nakamura, S. (2001) *Biochem. Biophys. Res. Commun.* **280**, 1085–1092
45. Ahn, B. H., Rhim, H., Kim, S. Y., Sung, Y. M., Lee, M. Y., Choi, J. Y., Wolozin, B., Chang, J. S., Lee, Y. H., Kwon, T. K., Chung, K. C., Yoon, S. H., Hahn, S. J., Kim, M. S., Jo, Y. H., and Min do, S. (2002) *J. Biol. Chem.* **277**, 12334–12342
46. Fridriksson, E. K., Shipkova, P. A., Sheets, E. D., Holowka, D., Baird, B., and McLafferty, F. W. (1999) *Biochemistry* **38**, 8056–8063
47. Brown, D. A., and London, E. (1998) *Annu. Rev. Cell Dev. Biol.* **14**, 111–136
48. Bussell, R., Jr., Ramlall, T. F., and Eliezer, D. (2005) *Protein Sci.* **14**, 862–872
49. Sharon, R., Bar-Joseph, I., Mirick, G. E., Serhan, C. N., and Selkoe, D. J. (2003) *J. Biol. Chem.* **278**, 49874–49881
50. Sharon, R., Goldberg, M. S., Bar-Josef, I., Betensky, R. A., Shen, J., and Selkoe, D. J. (2001) *Proc. Natl. Acad. Sci. U. S. A.* **98**, 9110–9115

Dopaminergic dysfunction in unrelated, asymptomatic carriers of a single parkin mutation

Rivka Inzelberg, Nobutaka Hattori and Yoshikuni Mizuno

Neurology 2005;65;1843-
DOI: 10.1212/01.wnl.0000200029.57187.05

Dopaminergic dysfunction in unrelated, asymptomatic carriers of a single parkin mutation

To the Editor: We read with interest the article by Khan et al.[1] The authors studied asymptomatic parkin heterozygotes by 18F-dopa PET and found a significant reduction of uptake in putamen, caudate, dorsal and ventral midbrain. An interesting observation relates to the subtle extrapyramidal symptoms in four of these "asymptomatic" carriers. The authors recommended follow-up to verify whether they develop parkin disease.

One of our patients with a single parkin mutation developed parkin disease 23 years after the manifestation of tremor as the only symptom. This 56-year-old man is the only child of nonconsanguineous parents of European Jewish origin. At age 13, left hand tremor was noticed. Tremor severity remained unchanged for 23 years (without treatment), until the age of 36, when he experienced prominent rest tremor and bradykinesia of the left limbs.

Five years later, L-dopa was initiated with excellent response. Dyskinesias occurred 3 years after L-dopa onset, necessitating a left pallidotomy 18 years later. Brain MRI was normal. Genetic testing revealed a heterozygous C to T transition at nucleotide position 1197 of parkin gene (exon 10).

Parkin disease presents as slowly progressive parkinsonism.[2,3] Even if significant dopaminergic dysfunction appears in PET studies of single parkin mutation carriers, other mechanisms and the amount of intact dopamine store at a young age might be compensatory to prevent early clinical expression.[1]

However, this explanation may only relate to some patients. Others might develop parkin disease earlier, as occurred in another of our sporadic patients who carries a single parkin mutation. This 36-year-old woman is the only child of nonconsanguineous parents of European Jewish origin. At the age of 31, she experienced left foot dystonia, slowing of her left hand accompanied by rest tremor, which later progressed to bilateral parkinsonism. Response to L-dopa given 5 years after disease onset was excellent. Brain MRI was normal. A heterozygous deletion of exon 7 of parkin was found.[4]

Haploinsufficiency (reduction in normal protein function) and dominant negative effects (nonfunctional polypeptide physically interferes with normal protein) proposed as causes of dopaminergic cell dysfunction[1] or the inhibition of parkin's ubiquitin 3 ligase activity by S-nitrosylation[5] are probably not the only explanations. Other genetic or environmental factors might predispose carriers of a single parkin mutation not only to late-onset but also to young-onset Parkinson disease.

Rivka Inzelberg, MD, Nobutaka Hattori, MD, Yoshikuni Mizuno, MD, *Hadera, Israel*

Editor's Note: The authors had the opportunity to respond to this Correspondence but declined.

References

1. Khan NL, Scherfler C, Graham E, et al. Dopaminergic dysfunction in unrelated, asymptomatic carriers of a single parkin mutation. Neurology 2005;64:134–136.
2. Nisipeanu P, Inzelberg R, Abo Mouch S, et al. Parkin gene causing benign autosomal recessive juvenile parkinsonism. Neurology 2001;56:1573–1576.
3. Inzelberg R, Hattori N, Nisipeanu P, et al. Camptocormia, axial dystonia, and parkinsonism: Phenotypic heterogeneity of a parkin mutation. Neurology 2003;60:1393–1394.
4. Inzelberg R, Nisipeanu P, Carasso RL, Blumen SC, Hattori N, Mizuno Y. Early-onset parkinsonism in heterozygous parkin mutation carriers. Ann Neurol 2004;56(suppl 8):S28.
5. Choung KKK, Thomas B, Li X, et al. S-nitrosylation of parkin regulates ubiquitination and compromises parkin's protective function. Science 2004;304:1328–1331.

fMRI reveals large-scale network activation in minimally conscious patients

To the Editor: We read Schiff et al.'s article with great interest.[1] We conducted a case study regarding the application of fMRI to a patient in a minimally conscious state.[2] The Schiff et al. article appears to corroborate our findings of multisensory and cognitive fMRI BOLD responses in an overtly unresponsive brain-injured patient. These initial reports probing the minimally conscious state with imaging methods offer intriguing possibilities, and indeed the 2001 fMRI case study closely correlated with the patient's eventual recovery. Further research in this area is warranted.

Chad H. Moritz, PhD, *Madison, WI*

To the Editor: Schiff et al.[1] reported that two severely brain-injured patients monitored with fMRI showed brain responses to auditory personal narratives but not when the input was presented in reverse, meaningless form. A similar study[3] with equally remarkable results was carried out more than 20 years earlier, ironically also by researchers at Columbia University. That it was overlooked by Schiff et al. is an indication of the obscurity into which this study has undeservedly fallen.

In the earlier report of Boyle and Greer, three brain-injured patients with disabilities at least as severe as those in the Schiff et al. study were examined. In place of monitoring by fMRI, operant conditioning was used to increase small spontaneous responses made by each patient including eyelid, finger, or mouth movements. The reinforcer in each case was the playing of a 15-second sample of music identified as the patient's favorite, presented contingent on an occurrence of the target response. A multiple-baseline design with reversal,[4] a technique of the field of applied behavior analysis, was used to assess causal relationships. The authors reported good evidence of learning for the first patient, lesser but suggestive evidence for the second, and little evidence of learning for the third.

The first patient subsequently recovered from the vegetative state to a limited extent, the second did not recover, and the third died within 1 week after the end of testing. Thus successful operant conditioning may possibly predict recovery and may even help produce it.

Schiff et al. concluded in their later study that their findings of changes in brain activity in response to meaningful auditory input "raise important questions related to whether MCS [minimally conscious state] patients have a greater capacity to experience subjective states but also to benefit from therapeutic intervention." The results of the Boyle and Greer study raise the same questions, but go one step further by showing an actual change in behavior in response to reinforcement by emotionally meaningful stimuli.

Although the methods differ, the results of the two studies complement each other. Both methods should be exploited as valuable tools towards the goals of understanding and enhancing the capabilities of the brain-injured, minimally conscious patient.

Stephen L. Black, PhD, *Lennoxville, Canada*

Editor's Note: The authors had the opportunity to respond but declined.

References

1. Schiff ND, Rodriguez-Moreno D, Kamal A, et al. fMRI reveals large-scale network activation in minimally conscious patients. Neurology 2005;64:514–523.
2. Moritz CH, Rowley HA, Haughton VM, Swartz KR, Jones J, Badie B. Functional MR imaging assessment of a non-responsive brain injured patient. Magn Reson Imaging 2001;19:1129–1132.
3. Boyle ME, Greer, RD. Operant procedures and the comatose patient. J Appl Behav Anal 1983;16:3–12.
4. Kazdin A. Behavior Modification in Applied Settings, 6th ed. Belmont, CA: Wadsworth; 2001.

Preserved Cardiac Sympathetic Nerve Accounts for Normal Cardiac Uptake of MIBG in PARK2

Satoshi Orimo, MD, PhD,[1]* Takeshi Amino, MD,[1]
Masayuki Yokochi, MD, PhD,[2]
Tohru Kojo, MD, PhD,[3] Toshiki Uchihara, MD, PhD,[3]
Atsushi Takahashi, MD, PhD,[4]
Koichi Wakabayashi, MD, PhD,[5]
Hitoshi Takahashi, MD, PhD,[6]
Nobutaka Hattori, MD, PhD,[7] and
Yoshikuni Mizuno, MD, PhD[7]

[1]Department of Neurology, Kanto Central Hospital, Tokyo, Japan; [2]Department of Neurology, Ebara Metropolitan Hospital, Tokyo, Japan; [3]Department of Neuropathology, Tokyo Metropolitan Institute for Neuroscience, Tokyo, Japan; [4]Organ and Function Pathology Division, Yokufukai Geriatric Hospital, Tokyo, Japan; [5]Department of Neuropathology, Hirosaki University School of Medicine, Hirosaki, Japan; [6]Department of Pathology, Brain Research Institute, University of Niigata, Niigata, Japan; [7]Department of Neurology, Juntendo University School of Medicine, Tokyo, Japan

Abstract: **We performed [^{123}I] MIBG myocardial scintigraphy in two of three patients with PARK2 from unrelated families and examined the heart tissues from the three patients immunohistochemically using an antibody against tyrosine hydroxylase (TH) to see whether cardiac sympathetic nerve is involved. Cardiac uptake of MIBG was normal except for a slight decrease in the late phase in one of the patients. Postmortem examination revealed that TH-immunoreactive nerve fibers in the epicardium were well preserved in all three patients. The present study confirmed that cardiac sympathetic nerve is well preserved in PARK2 with a homozygous exon deletion, which accounts for normal cardiac uptake of MIBG. Moreover, normal cardiac uptake of MIBG might be of potential diagnostic value to indicate the absence of Lewy body pathology, even in patients with levodopa-responsive Parkinsonism, as in PARK2.** © 2005 Movement Disorder Society

Key words: PARK2; Parkinson's disease; MIBG myocardial scintigraphy; cardiac sympathetic nerve; denervation

*Correspondence to: Dr. Satoshi Orimo, Department of Neurology, Kanto Central Hospital, 6-25-1 Kami-Yoga, Setagaya-ku, 158-8531 Tokyo, Japan. E-mail: orimo@kanto-ctr-hsp.com

Received 24 December 2004; Revised 27 January 2005; Accepted 31 January 2005

Published online 6 July 2005 in Wiley InterScience (www.interscience.wiley.com). DOI: 10.1002/mds.20594

PARK2 is an autosomal recessive inherited form of familial Parkinsonism caused by mutations of *parkin*,[1] a gene that maps to chromosome 6q25-q27,[2] and is characterized by early onset of the disease usually before the age of 40 years, dystonia, hyperreflexia, sleep benefit, early complications from levodopa treatment, and slow progression.[3] Neuropathological findings of PARK2 are characterized by generalized loss of neurons in the substantia nigra pars compacta and locus coeruleus with no Lewy bodies.[4–6] PARK2 can be differentiated from idiopathic Parkinson's disease (PD) by means of early onset of the disease and other characteristics described above. However, it is sometimes difficult to differentiate PD from PARK2, because some patients with PARK2 develop clinical features after the age of 40 years.[7,8]

Decreased cardiac uptake of *meta*-iodobenzylguanidine (MIBG) on [^{123}I] MIBG myocardial scintigraphy, which indicates cardiac sympathetic denervation, has been reported in patients with PD. This imaging approach might be a new diagnostic tool to differentiate PD from other movement disorders with similar symptomatology such as multiple system atrophy (MSA), progressive supranuclear palsy (PSP), and corticobasal degeneration (CBD).[9–13] Cardiac sympathetic denervation in PD was also reported by means of decreased cardiac uptake of 6-[^{18}F] fluorodopamine on positron emission tomography.[14] Recently, we reported depletion of cardiac sympathetic nerve in patients with PD but not in patients with MSA, which accounted for the difference in cardiac uptake of MIBG between PD and MSA.[15,16] In contrast, cardiac uptake of MIBG has been reported to be normal in patients with autosomal recessive juvenile Parkinsonism[17] and a single patient with PARK2.[18] Therefore, [^{123}I] MIBG myocardial scintigraphy might be a useful diagnostic tool to differentiate PARK2 from PD.

In the present report, we studied three genetically and pathologically confirmed patients with PARK2 from unrelated families to see whether cardiac sympathetic nerve was involved by means of [^{123}I] MIBG myocardial scintigraphy and pathological examination.

PATIENTS AND METHODS

Patient 1

A 73-year-old man with PARK2 with a homozygous exon 4 deletion in the *parkin* gene developed a tremor in both hands at the age of 24, followed by gait disturbance. These features responded well to levodopa. He had no autonomic symptoms, and he had no signs such as orthostatic hypotension (OH), severe constipation, and frequency of urination. His parents were consanguineous

and his younger brother and two younger sisters had been diagnosed as having PARK2. A single photon computed tomography (SPECT) of [^{123}I] MIBG myocardial scintigraphy at the age of 70, 46 years after the onset, showed normal cardiac uptake of MIBG in both the early (Fig. 1A) and the late phase. Heart-to-mediastinum (H/M) ratio of the early and late phase was 2.28 and 2.30, respectively. That of the early and late phase of age-matched control (8 men and 6 women; 59–81; 71.9 ± 6.6 years of age) was 2.20 ± 0.15 and 2.14 ± 0.19, respectively. Postmortem examination 3 hr after death revealed loss of pigmented neurons and gliosis in the substantia nigra pars compacta and locus coeruleus with no Lewy body pathology.

Patient 2

A 66-year-old man with PARK2 with a homozygous exon 4 deletion in the *parkin* gene developed a tremor, rigidity, and gait disturbance at the age of 28. These features responded well to levodopa. He had no autonomic symptoms or signs. He had hypertension with no antihypertensive medications. A SPECT of [^{123}I] MIBG myocardial scintigraphy at the age of 63 years, 35 years after the onset, showed normal cardiac uptake of MIBG in the early phase (Fig. 1B) and a slight decrease in the late phase. H/M ratio of the early and the late phase was 1.98 and 1.69, respectively. Postmortem examination 2 hr after death revealed loss of pigmented neurons and gliosis in the substantia nigra pars compacta and locus coeruleus with no Lewy body pathology. The weight of the heart was 400 gm and a histological examination was unremarkable.

Patient 3

A 70-year-old man with PARK2 with a homozygous exon 4 deletion in the *parkin* gene had been reported clinically and neuropathologically elsewhere.[6] Briefly, he developed a dystonic gait at the age of 32, followed by hand tremor, rigidity, bradykinesia, and postural instability. These features responded well to levodopa. He had no OH but had constipation and frequency of urination 2 years before his death. Postmortem examination 4 hr after death revealed loss of pigmented neurons and gliosis in the substantia nigra pars compacta and locus coeruleus with no Lewy body pathology.

Methods

We immunohistochemically examined the heart tissues using an antibody against tyrosine hydroxylase (TH), a rate-limiting enzyme of catecholamine biosynthesis. The anterior wall of the left ventricle of the heart was selected based on previous studies[15,16] because TH-immunoreactive nerve fibers were more numerous in the anterior than in the posterior wall of the ventricle[19] and cardiac uptake of MIBG is mainly observed in the left ventricle. The blocks from Patients 1, 2, and 3 and three patients with neuropathologically confirmed Lewy body pathology-positive PD as well as three control subjects (Table 1) were fixed with formalin and embedded in paraffin. Deparaffinized sections were stained with hematoxylin and eosin (H&E) or immunostained with a monoclonal antibody against TH (Sigma, St. Louis, MO; dilution 1:5,000) by the avidin–biotin–peroxidase complex method with Vectastain kit (Vector, Burlingame, CA). The peroxidase labeling was visualized with diaminobenzidine-nickel as chromogen. The number of TH-immunoreactive nerve fibers in the epicardium was assessed according to a semiquantitative rating scale: −, absent or nearly absent; +, sparse; ++, moderate; +++, numerous.

RESULTS

The clinical characteristics and TH immunopositivity are shown in Table 1. On routine HE staining, no abnormal findings were found in either the myocardium or the epicardium of each patient and control subjects. There were moderate to numerous TH-immunoreactive nerve fibers in the epicardium from all the patients with PARK2 (Fig. 2A–C, Table 1) as well as from control subjects (Fig. 2E, Table 1). In contrast, the number of TH-immunoreactive nerve fibers was absent or nearly absent in the epicardium from all the patients with PD (Fig. 2D, Table 1).

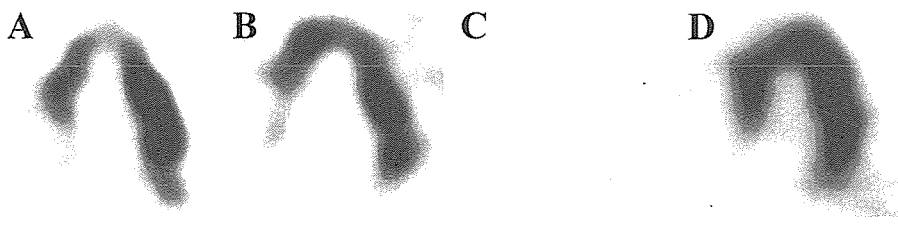

FIG. 1. Long axis of SPECT images of two patients with PARK2, a patient with PD (67 years of age; female; duration of illness, 3 years) and a control subject (64 years of age; female). Cardiac uptake of MIBG of the patients with PARK2 is normal (**A** and **B**) as well as that of the control subject (**D**). In contrast, that of the patient with PD is severely decreased (**C**).

TABLE 1. *Clinical characteristics, H/M ratio, and TH immunopositivity*

Patient	Diagnosis	Age (yr)	Sex	Duration (yr)	Type of mutation (deletion)	H/M (early)	TH
1	PARK2	73	M	49	Exon 4	2.28	++~+++
2	PARK2	66	M	38	Exon 4	1.98	+++
3	PARK2	70	M	38	Exon 4		++~+++
4	PD	70	M	10			−
5	PD	82	F	10			−
6	PD	91	F	15			−
C1	Peritonitis	81	F				+++
C2	Colon cancer	86	M				+++
C3	Esophageal cancer	89	F				+++

TH, tyrosine hydroxylase; PD, Parkinson's disease.

DISCUSSION

The present patients had typical PARK2 clinical characteristics such as early onset, effectiveness of levodopa treatment, and long duration of illness. Autonomic symptoms and signs were absent or very mild in all the patients. They all had the *parkin* gene mutation, a homozygous exon 4 deletion, and were diagnosed as having PARK2.

Decreased cardiac uptake of MIBG or fluorodopamine in PD has been reported.[9–14] Cardiac uptake of fluorodopamine is also decreased in patients with familial Parkinsonism as seen in PARK1 (linked to a mutant form of α-synuclein) or in PARK4 (overproduction of normal α-synuclein) patients, who have OH and Lewy body pathology.[20] Our patients with PARK2, who have neither OH nor Lewy body pathology, showed normal cardiac uptake of MIBG except for a slight decrease in the late phase in one of the patients, in spite of the fact that the duration of this patient's was over 30 years. Although this slight decrease in the late phase may represent early involvement of cardiac sympathetic nerve,[10,12] it is attributable to increased exocytosis due to hypertensive heart disease.[21] The present findings and a previous report,[18] even considering the limited number of patients, strongly suggest that cardiac uptake of MIBG is a useful diagnostic marker to differentiate PARK2 from PD. Moreover, the present findings indicate that normal cardiac uptake of MIBG is associated with the absence of Lewy body pathology and that, in turn, the decease in cardiac uptake of MIBG is closely related to the presence of Lewy body pathology. This assumption is further supported by well-preserved TH-immunoreactive nerve fibers, which is presumably cardiac sympathetic nerve,[16] in the epicardium of our three patients with PARK2. This is in sharp contrast with patients with PD, who have decreased cardiac uptake of MIBG, depletion of cardiac sympathetic nerve, and Lewy body pathology. It might be worth mentioning that patients with familial Parkinsonism caused by inherited α-synucleinopathies had OH from sympathetic failure, whereas none of the patients with PARK2 had OH. This finding provides indirect support for a contribution of sympathetic denervation to OH in PD.

In conclusion, the present study confirmed that cardiac sympathetic nerve is well preserved in PARK2 with homozygous exon deletion, which accounts for normal cardiac uptake of MIBG. Moreover, normal cardiac uptake of MIBG might be of potential diagnostic value to indicate the absence of Lewy body pathology.

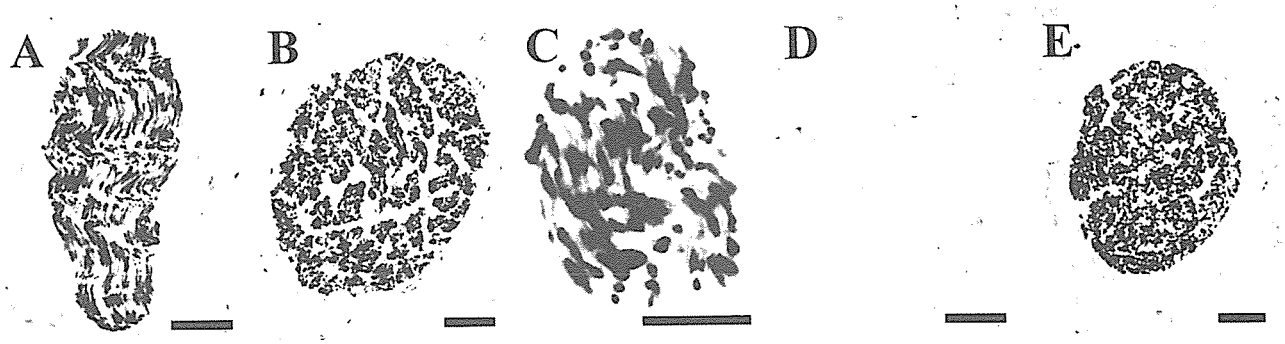

FIG. 2. Tyrosine hydroxylase (TH) immunostaining of the epicardium in the patients with PARK2 (**A–C**), the patient with PD (**D**), and the control subject (**E**). TH-immunoreactive nerve fibers are well preserved in the epicardium from the patient with PARK2 (A–C) and control subject (E), whereas those from the patient with PD (D) are absent. Scale bar = 20 μm.

Acknowledgments: This study was supported by the Japan Foundation for Neuroscience and Mental Health (Tama Nakagawa Foundation). We thank Dr. M. Takahashi for his helpful suggestion and Ms. Nakamura for her technical assistance.

REFERENCES

1. Kitada T, Asakawa S, Hattori N, et al. Mutations in the parkin gene cause autosomal recessive juvenile Parkinsonism. Nature 1998; 392:605–608.
2. Matsumine H, Saito M, Shimoda-Matsubayashi S, et al. Localization of a gene for an autosomal recessive form of juvenile Parkinsonism to chromosome 6q25.2-27. Am J Hum Genet 1997;60: 588–596.
3. Ishikawa A, Tsuji S. Clinical analysis of 17 patients in 12 Japanese families with autosomal-recessive type juvenile parkinsonism. Neurology 1996;47:160–166.
4. Takahashi H, Ohama E, Suzuki S, et al. Familial juvenile Parkinsonism: clinical and pathological study in a family. Neurology 1994;44:437–441.
5. Mori H, Kondo T, Yokochi M, et al. Pathological and biochemical studies of juvenile parkinsonism linked to chromosome 6p. Neurology 1998;51:890–892.
6. Hayashi S, Wakabayashi K, Ishikawa A, et al. An autopsy case of autosomal-recessive juvenile Parkinsonism with a homozygous exon 4 deletion in the *parkin* gene. Mov Disord 2000;15:884–888.
7. Tassin L, Durr A, de Broucker T, et al. Chromosomal 6-linked autosomal recessive early-onset parkinsonism: linkage in European and Algerian families, extension of the clinical spectrum, and evidence of a small homozygous deletion in one family—the French Parkinson's Disease Genetics Study Group, and the European Consortium on Genetic Susceptibility in Parkinson's Disease. Am J Hum Genet 1998;63:88–94.
8. Klein C, Plamstaller PP, Kis B, et al. Parkin deletion in a family with adult-onset, tremor-dominant Parkinsonism: expanding the phenotype. Ann Neurol 2000;48:65–71.
9. Yoshita M. Differentiation of idiopathic Parkinson's disease from striatonigral degeneration and progressive supranuclear palsy using iodine-123 meta-iodobenzylguanidine myocardial scintigraphy. J Neurol Sci 1998;155:60–67.
10. Orimo S, Ozawa E, Nakade S, Sugimoto T, Mizusawa H. ^{123}I-metaiodobenzylguanidine myocardial scintigraphy in Parkinson's disease. J Neurol Neurosurg Psychiatry 1999;67:189–194.
11. Braune S, Reinhardt M, Schnitzer R, Riedel A, Lücking CH. Cardiac uptake of [^{123}I] MIBG separates Parkinson's disease from multiple system atrophy. Neurology 1999;53:1020–1025.
12. Taki J, Nakajima K, Hwang E-H, et al. Peripheral sympathetic dysfunction in patients with Parkinson's disease without autonomic failure is heart selective and disease specific. Eur J Nucl Med 2000;27:566–573.
13. Orimo S, Ozawa E, Nakade S, et al. [^{123}I] MIBG myocardial scintigraphy differentiates corticobasal degeneration from Parkinson's disease. Intern Med 2003;42:127–128.
14. Goldstein DS, Holmes C, Li S-T, Bruce S, Metman LV, Cannon RO III. Cardiac sympathetic denervation in Parkinson disease. Ann Intern Med 2000;133:338–347.
15. Orimo S, Oka T, Miura H, et al. Sympathetic cardiac denervation in Parkinson's disease and pure autonomic failure but not in multiple system atrophy. J Neurol Neurosurg Psychiatry 2002;73: 776–777.
16. Amino T, Orimo S, Itoh Y, Takahashi A, Uchihara T, Mizusawa H. Profound cardiac sympathetic denervation occurs in Parkinson disease. Brain Pathol 2005;15:29–34.
17. Kitami T, Nomoto T, Nagao T, et al. ^{123}I-MIBG myocardial scintigraphy in juvenile Parkinsonism. Mov Disord 1998; 13(Suppl. 2):247.
18. Suzuki M, Hattori N, Orimo S, et al. Preserved myocardial ^{123}I-metaiodo-benzylguanidine uptake in autosomal recessive juvenile Parkinsonism: first case report. Mov Disord 2005;20:634–636.
19. Kawano H, Okada R, Yano K. Histological study on the distribution of autonomic nerves in the human heart. Heart Vessels 2003; 18:32–39.
20. Singleton A, Gwinn-Hardy K, Sharabi Y, et al. Association between cardiac denervation and Parkinsonism caused by α-synuclein gene triplication. Brain 2004;127:768–772.
21. Mitani I, Sumita S, Takahashi N, Ochiai H, Ishii M. ^{123}I-MIBG myocardial imaging in hypertensive patients: abnormality progresses with left ventricular hypertrophy. Ann Nucl Med 1996; 10:315–321.

Hum Genet (2005) 117: 520–527
DOI 10.1007/s00439-005-1342-8

ORIGINAL INVESTIGATION

Masayuki Ide · Kazuo Yamada · Tomoko Toyota
Yoshimi Iwayama · Yuichi Ishitsuka · Yoshio Minabe
Kazuhiko Nakamura · Nobutaka Hattori
Takashi Asada · Yoshikuni Mizuno · Norio Mori
Takeo Yoshikawa

Genetic association analyses of *PHOX2B* and *ASCL1* in neuropsychiatric disorders: evidence for association of *ASCL1* with Parkinson's disease

Received: 15 March 2005 / Accepted: 2 May 2005 / Published online: 14 July 2005

Abstract We previously identified frequent deletion/insertion polymorphisms in the 20-alanine homopolymer stretch of *PHOX2B* (*PMX2B*), the gene for a transcription factor that plays important roles in the development of oculomotor nerves and catecholaminergic neurons and regulates the expression of both tyrosine hydroxylase and dopamine β-hydroxylase genes. An association was detected between gene polymorphisms and overall schizophrenia, and more specifically, schizophrenia with ocular misalignment. These prior results implied the existence of other schizophrenia susceptibility genes that interact with *PHOX2B* to increase risk of the combined phenotype. *ASCL1* was considered as a candidate interacting partner of *PHOX2B*, as ASCL1 is a transcription factor that co-regulates catecholamine-synthesizing enzymes with PHOX2B. The genetic contributions of *PHOX2B* and *ASCL1* were examined separately, along with epistatic interactions with broader candidate phenotypes. These phenotypes included not only schizophrenia, but also bipolar affective disorder and Parkinson's disease (PD), each of which involve catecholaminergic function. The current case-control analyses detected nominal associations between polyglutamine length variations in *ASCL1* and PD ($P = 0.018$), but supported neither the previously observed weak association between *PHOX2B* and general schizophrenia, nor other gene-disease correlations. Logistic regression analysis revealed the effect of *ASCL1* dominant × *PHOX2B* additive ($P = 0.008$) as an epistatic gene–gene interaction increasing risk of PD. ASCL1 controls development of the locus coeruleus (LC), and accumulating evidence suggests that the LC confers protective effects against the dopaminergic neurodegeneration inherent in PD. The present genetic data may thus suggest that polyglutamine length polymorphisms in *ASCL1* could influence predispositions to PD through the fine-tuning of LC integrity.

M. Ide and K. Yamada contributed equally to this work

M. Ide · K. Yamada · T. Toyota · Y. Iwayama · Y. Ishitsuka
T. Yoshikawa (✉)
Laboratory for Molecular Psychiatry,
RIKEN Brain Science Institute, 2-1 Hirosawa,
Wako-city, Saitama 351-0198, Japan
E-mail: takeo@brain.riken.go.jp
Tel.: +81-48-4675968
Fax: +81-48-4677462

Y. Minabe · K. Nakamura · N. Mori
Department of Psychiatry and Neurology,
Hamamatsu University School of Medicine,
Hamamatsu 431-3192, Japan

N. Hattori · Y. Mizuno
Department of Neurology,
Juntendo University School of Medicine,
Tokyo 113-8421, Japan

T. Asada
Department of Psychiatry,
University of Tsukuba School of Medicine, Ibaraki 305-8576,
Japan

Introduction

Paired-like homeobox 2b (PHOX2B, also known as PMX2B or NBPhox) is a homeodomain transcription factor, and is known to determine noradrenergic phenotype (Pattyn et al. 2000) and play a role in the development of cranial motor nerves, including the oculomotor (nIII) and trochlear (nIV) nerves (Pattyn et al. 1997) controlling ocular alignment and movement. As a transcription factor, PHOX2B regulates the expression of tyrosine hydroxylase (TH) and dopamine β-hydroxylase (DBH) genes. TH catalyzes the conversion of L-tyrosine to L-dihydroxyphenylalanine (L-DOPA), a precursor of dopamine, and DBH catalyzes the conversion of dopamine to noradrenaline. The protein structure of PHOX2B is characterized by two

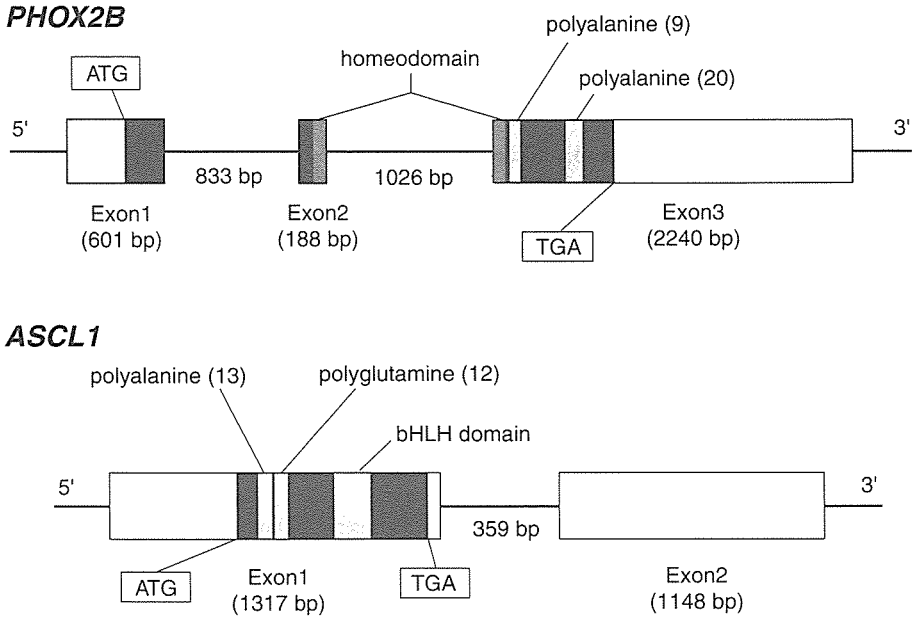

Fig. 1 Schematic representation of the *PHOX2B* (NM_003924) (*above*) and *ASCL1* (NM_004316) genes (*below*). Exons are *boxed*, and initiation and stop codons and protein domains are indicated

homopolymeric stretches of alanine residues: one consisting of nine alanines located downstream of the homeodomain; the other comprising 20 alanines (Ala20) on the C-terminal side (Fig. 1). Our prior genomic screening of *PHOX2B* identified frequent length variations in the Ala20 stretch in the general population, representing an unusual phenomenon compared with other polyalanine-containing transcription factors (Toyota et al. 2004). Variations included −3Ala, −5Ala, −7Ala, −13Ala and +2Ala. These alterations in alanine length resulted in decreased transcriptional ability of the protein and represented the only functional polymorphisms found in the gene. In accordance with the known function of PHOX2B and the functional consequences of these variations, associations between the polymorphisms and general schizophrenia were detected, particularly for schizophrenia manifesting with strabismus (ocular misalignment) (Toyota et al. 2004). That study also raised a possibility of interactions between *PHOX2B* and other schizophrenia-precipitating factors (genes) for increased risk of the combined phenotype (Toyota et al. 2004).

Human achaete-scute homologue 1 (HASH1; ASCL1 in HUGO nomenclature), a human orthologue of mouse Mash1, is a basic helix–loop–helix (bHLH) transcription factor that is known to co-regulate differentiation of the autonomic system along with PHOX2B (Pattyn et al. 2000). Cross-regulation by the *Phox2* and *Mash1* genes, and the importance of the HASH1-PHOX pathway in the development of neurons in the noradrenergic lineage have been demonstrated in both mice (Pattyn et al. 1999, 2000), and a human disease mechanism (De Pontual et al. 2003). We therefore speculated that *PHOX2B* and *ASCL1* may affect predispositions to broad catecholamine-related diseases both separately and in combination. The present study examined genetic associations between *PHOX2B* and *ASCL1* and schizophrenia, bipolar disorder and Parkinson's disease (PD).

Materials and methods

Study subjects

Subjects included 715 schizophrenic patients (394 men, mean age 48.3 ± 12.3 years; 321 women, mean age 50.7 ± 13.3 years), 249 bipolar disorder patients (118 men, mean age 52.6 ± 13.2 years; 131 women, mean age 55.8 ± 12.9 years), 100 PD patients (32 men, mean age 67.3 ± 7.8 years; 68 women, mean age 67.8 ± 7.0 years) and 801 healthy controls (369 men, mean age 40.9 ± 11.4 years; 432 women, mean age 41.3 ± 13.7 years). Compared with the prior study (Toyota et al. 2004), the number of schizophrenia patients was increased by 369 and the number of controls was increased by 260, but these newly added subjects were not screened for strabismus. All subjects were recruited from a geographic area located in central Japan. Diagnosis of schizophrenia and bipolar disorder was based on the *Diagnostic and statistical manual of mental disorders* (American Psychiatric Association 1994). PD was diagnosed according to the standardized criteria. All PD patients underwent brain computed tomography examination to exclude organic abnormalities. Control subjects were recruited from hospital staff and company employees who were documented as free of psychoses or any kind of neurodegenerative disorder. None of the current subjects displayed mental retardation or congenital central hypoventilation syndrome (De Pontual et al. 2003). This study was approved by the Ethics Commit-

tees of RIKEN, Hamamatsu University and Juntendo University, and all subjects provided written informed consent to participate.

Mutation screening of *ASCL1*

ASCL1 is located on human chromosome 12q22-q23 (Renault et al. 1995) and comprises two exons, with the first exon including both the initiation and stop codons (Fig. 1). The protein-coding region contains a poly-alanine stretch comprising 13 alanines, and a polyglutamine tract of 12 glutamine residues (Gln12), in addition to the bHLH. The two exons and their flanking genomic stretches were screened using polymerase chain reaction (PCR) amplification and subsequent direct sequencing of genomic DNA from 24 randomly chosen patients. Sequencing was performed using a DYEnamic ET terminator cycle sequencing kit (Amersham, Piscataway, N.J., USA). Information on primer sequences and PCR conditions employed in this study is available on request. Screening detected the insertion of three CAG repeats (coding glutamine) into the polyglutamine stretch. This was the only non-synonymous polymorphism identified, and we therefore focused on this Gln12 length polymorphism in subsequent analyses.

Genotyping

Genotyping of Ala20 length variations in the *PHOX2B* was performed according to the methods described elsewhere (Toyota et al. 2004). To genotype Gln12 polyglutamine length variations in *ASCL1*, template DNA was amplified using fluorescently labeled forward (5′-AGCTCTGCCAAGATGGAGAG; 3′ end at nt c.26) and reverse (5′- gtttcttTTGCTTGGGCGC-TGACTTGT; 3′ end at nt c.236) primers. The *underlined* tail sequence was added because Taq DNA polymerase catalyzes the non-templated addition of adenosine to the 3′ end of PCR products to varying degrees. This phenomenon is primer-specific and represents a potential source of genotyping error. Placing the gtttctt sequence at the 5′ end of reverse primers produces nearly 100% adenylation of the 3′ end of the forward strand, facilitating accurate genotyping (Brownstein et al. 1996; Itokawa et al. 2003). PCR products were run on an ABI 3700 genetic analyzer (Applied Biosystems, Foster City, Calif., USA), and the resulting data were analyzed using GeneScan software (Applied Biosystems). Genotypes were confirmed by subcloning the amplicons into a TA vector (Invitrogen, Carlsbad, Calif., USA) and sequencing. Primers were designed to produce a 249-bp DNA fragment for the wild-type allele (Gln12), but GeneScan analysis yielded a band approximately 14 bp shorter than expected (Fig. 2a), with occasional inconsistent genotype results compared with those obtained by subcloning, which could not be resolved by applying the constant 14-bp difference to GeneScan results. This phenomenon was attributed to the secondary DNA structure generated by abundant GCs in the PCR products (Toyota et al. 2004). When 7-deaza-2′-deoxyguanosine triphosphate (c^7 dGTP) was added to the PCR reaction mixture (c^7 dGTP:dGTP = 1:3) to breakdown hydrogen bonds in the GC-rich templates, GeneScan peaks were broadened and two adjacent peaks merged (Fig. 2b). We replaced all dGTP in the PCR reaction mixture with c^7 dGTP, and obtained sharp and correctly sized bands, enabling accurate genotyping (Fig. 2c).

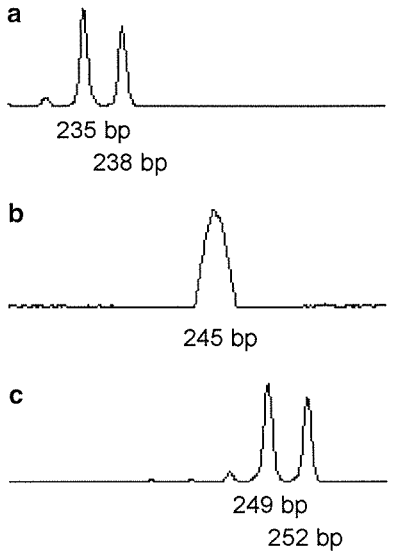

Fig. 2a–c GeneScan migration patterns of *ASCL1* Gln12 length polymorphisms. DNA fragments with Gln12 or Gln13 genotypes were run after PCR under varying concentrations of c^7 dGTP. Exact sizes of the Gln12 and Gln13 alleles were 249 and 252 bp, respectively. **a** The c^7 dGTP was not added to the PCR mixture. Note that displayed allele sizes were 14 bp shorter than actual sizes. **b** Addition of c^7 dGTP to 25% resulted in fusion of the two peaks. **c** When all dGTP in the PCR reaction mixture was replaced with c^7dGTP, peaks appeared at expected sizes with good separation of the two adjacent alleles

Statistical analysis

Associations of either *PHOX2B* or *ASCL1* polymorphisms with each neuropsychiatric disorder were evaluated using the Monte–Carlo method implemented in the CLUMP program (T1–T4 modes; number of simulations set to 10,000; random number seed, 100) (Sham and Curtis 1995) or Fisher's exact test when appropriate. Rare alleles or genotypes showing frequencies of < 1% in both comparison groups were removed from the analysis. Hardy–Weinberg equilibrium was evaluated using Arlequin software (http://lgb.unige.ch/arlequin/) (Schneider and Excofier 2000). Logistic regression analysis in the SPSS Regression Models software (SPSS Japan, Tokyo, Japan) was performed to test the joint

effects of the two genes. Letting P represent the probability of an individual being a case rather than a control, we modeled P as

$$\log it(P) = \beta_0 + \sum_{i=1}^{4} \beta_i x_i + \sum_{i=1}^{2} \sum_{j=3}^{4} \beta_{ij} x_i x_j$$

where x_1, x_2, x_3 and x_4 represent covariants depending on the genotypes of the individual, β_0 is the intercept, and β_i and β_{ij} are coefficients to be estimated. When applied to the formula, genotypes were dichotomized into two groups: wild-type (w); and mutant (m). Following the approach of Cordell and Clayton (2002) for the possible genotypes of w/w, m/w and m/m, we coded -1, 0 and 1, respectively, to represent the additive effects of allele m and -0.5, 0.5, -0.5, respectively, to represent the dominant effect of allele m over allele w.

Results

Table 1 shows the results of association analyses between *PHOX2B* Ala20 length polymorphisms and the three disease categories. We detected six different genotypes, and distributions of genotypes in each group were all in Hardy–Weinberg equilibrium. None of the modes T1–T4 on CLUMP analysis displayed significant associations for any disease groups. The number of different alleles observed in this study was the same as in our previous study (Toyota et al. 2004), although much larger cohorts were examined here. Again, no allelic associations were detected for any of the three neuropsychiatric disorders.

Tables 2 and 3 show the results of genotypic and allelic analyses of *ASCL1* Gln12 stretch polymorphisms, respectively. Analysis of the 1,866 subjects yielded 13 different length variations in the Gln12 homopolyer repeat region of *ASCL1*. These polymorphisms were not genotypically associated with schizophrenia or bipolar disorder, but displayed associations with PD ($P < 0.05$ in T2, T3 and T4) (Table 2). Allelic analysis demonstrated that the allele containing 12 glutamine repeats, the most common of these alleles, was more frequent in PD than in the control group (2×2 Fisher's exact test, two-sided, $P = 0.015$; odds ratio = 1.68, 95% CI = 1.10–2.54), while the allele containing 15 glutamine repeats, as the second most common allele, exhibited an opposite distribution pattern ($P = 0.011$; odds ratio = 0.57, 95% CI = 0.36–0.89) (Table 3). These results suggest that the *ASCL1* allele harboring 15 glutamine repeats may play a protective role against PD manifestation.

Logistic regression analysis was then performed to test the joint effect of the two genes on PD. The Ala20 allele of *PHOX2B* and the Gln12 allele of *ASCL1* were classified as w, with the remaining alleles as m. As a result, only the effect of *ASCL1* dominant × *PHOX2B* additive was found to be significant ($P = 0.008$), among the effects of all possible interaction modes (Table 4).

Discussion

PHOX2B/ASCL1 and psychiatric disorders

We have previously reported genotypic associations between Ala20 polymorphisms in *PHOX2B* and overall

Table 1 Genotypic and allelic distributions of the *PHOX2B* Ala20 repeat polymorphism

	Schizophrenia ($n = 715$)	Bipolar disorder ($n = 249$)	Parkinson's disease ($n = 100$)	Controls ($n = 802$)
Genotype[a]	Genotype counts (% frequency)			
15/15	0 (0)	0 (0)	1 (1.0)	3 (0.4)
20/7	1 (0.2)	0 (0)	0 (0)	0 (0)
20/13	6 (0.9)	2 (1.2)	0 (0)	7 (0.9)
20/15	57 (8.8)	14 (8.4)	9 (9.3)	59 (7.4)
20/20	579 (89.8)	151 (90.4)	87 (89.7)	727 (91.2)
20/22	2 (0.3)	0 (0)	0 (0)	1 (0.1)
P[b,c]				
T1	0.35	0.81	0.50	
T2	0.50	0.76	0.71	
T3	0.54	0.83	0.60	
T4	0.46	0.89	0.79	
Allele[a]	Allele counts (% frequency)			
7	1 (0.1)	0 (0)	0 (0)	0 (0)
13	6 (0.5)	2 (0.6)	0 (0)	7 (0.4)
15	57 (4.4)	14 (4.2)	11 (5.7)	65 (4.1)
20	1224 (94.9)	318 (95.2)	183 (94.3)	1521 (95.4)
22	2 (0.2)	0 (0)	0 (0)	1 (0.1)
P[b,d]	0.64	0.88	0.34	

[a]Number of alanine repeats
[b]Minor genotypes and alleles with frequencies (< 1% in both comparison groups were omitted from analyses
[c]Calculated using the Monte Carlo method
[d]Calculated using Fisher's exact test

Table 2 Genotypic distribution of the *ASCL1* Gln12 repeat polymorphism

	Schizophrenia ($n=715$)	Bipolar disorder ($n=249$)	Parkinson's disease ($n=100$)	Controls ($n=802$)
Genotype[a]	Genotype counts (% frequency)			
6/12	1 (0.1)	0 (0)	0 (0)	0 (0)
6/15	1 (0.1)	0 (0)	0 (0)	0 (0)
7/12	0 (0)	0 (0)	0 (0)	1 (0.1)
8/12	0 (0)	0 (0)	0 (0)	1 (0.1)
9/12	1 (0.1)	0 (0)	0 (0)	2 (0.3)
9/15	1 (0.1)	0 (0)	0 (0)	0 (0)
11/12	1 (0.1)	0 (0)	0 (0)	1 (0.1)
12/12	429 (61.5)	144 (60.0)	74 (75.5)	481 (61.0)
12/13	21 (3.0)	8 (3.3)	3 (3.1)	21 (2.7)
12/14	2 (0.3)	0 (0)	1 (1.0)	1 (0.1)
12/15	186 (26.6)	66 (27.5)	16 (16.3)	232 (29.4)
12/16	6 (0.9)	4 (1.7)	0 (0)	8 (1.0)
12/17	2 (0.3)	0 (0)	0 (0)	1 (0.1)
12/18	0 (0)	0 (0)	0 (0)	1 (0.1)
12/19	1 (0.1)	0 (0)	0 (0)	1 (0.1)
13/13	1 (0.1)	0 (0)	0 (0)	0 (0)
13/15	9 (1.3)	3 (1.3)	1 (1.0)	3 (0.4)
14/15	1 (0.1)	0 (0)	0 (0)	0 (0)
15/15	34 (4.9)	14 (5.8)	3 (3.1)	31 (3.9)
15/16	1 (0.1)	0 (0)	0 (0)	3 (0.4)
15/17	0 (0)	1 (0.4)	0 (0)	0 (0)
$P^{b,c}$				
T1	0.41	0.50	0.052	
T2	0.28	0.33	*0.016*	
T3	0.25	0.61	*0.010*	
T4	0.33	0.39	*0.046*	

[a] Number of glutamine repeats
[b] Minor genotypes and alleles with frequencies < 1% in both comparison groups were omitted from analyses
[c] Calculated using the Monte Carlo method

schizophrenia ($P=0.012$), with a more prominent association for schizophrenia with strabismus ($P=0.004$) (Toyota et al. 2004). However, the present study did not detect this association in a larger case-control panel with a 2.2-fold increase in the schizophrenia population and a 1.6-fold increase in control samples. This discrepancy may be partly due to the fact that prior control samples had undergone ocular examinations, and only those subjects who did not suffer from strabismus were chosen, while the present study used control samples with-

Table 3 Allelic distribution of the *ASCL1* Gln12 repeat polymorphism

	Schizophrenia ($n=715$)	Bipolar disorder ($n=249$)	Parkinson's disease ($n=100$)	Controls ($n=802$)
Allele[a]	Allele counts (% frequency)			
6	2 (0.1)	0 (0)	0 (0)	0 (0)
7	0 (0)	0 (0)	0 (0)	1 (0.1)
8	0 (0)	0 (0)	0 (0)	1 (0.1)
9	2 (0.1)	0 (0)	0 (0)	2 (0.1)
11	1 (0.1)	0 (0)	0 (0)	1 (0.1)
12	1079 (77.3)	366 (76.3)	168 (85.7)	1232 (78.2)
13	32 (2.3)	11 (2.3)	4 (2.0)	24 (1.5)
14	3 (0.2)	0 (0)	1 (0.5)	1 (0.1)
15	267 (19.1)	98 (20.4)	23 (11.7)	300 (19.0)
16	7 (0.5)	4 (0.8)	0 (0)	11 (0.7)
17	2 (0.1)	1 (0.2)	0 (0)	1 (0.1)
18	0 (0)	0 (0)	0 (0)	1 (0.1)
19	1 (0.1)	0 (0)	0 (0)	1 (0.1)
$P^{b,c}$				
T1	0.30	0.40	*0.036*	
T2	0.29	0.40	*0.022*	
T3	0.27	0.51	*0.018*	
T4	0.27	0.51	*0.026*	

[a]Number of glutamine repeats
[b]Minor genotypes and alleles with frequencies < 1% in both comparison groups were omitted from analyses
[c]Calculated using the Monte Carlo method

Table 4 Logistic regression analysis of effects of *PHOX2B* and *ASCL1* genes on Parkinson's disease

Variable	β[a]	SE[b]	Wald[c]	df[d]	*P*	Exp (β)[e]	95% CI[f]
ASCL1 dominant by *PHOX2B* additive	0.71	±0.27	7.0	1	0.008	2.0	1.2–3.4

[a]Logistic regression coefficient in the model
[b]Standard error of the coefficient
[c]Wald statistic to test significance of the coefficient
[d]Degrees of freedom for the Wald chi-square test
[e]Exponentiation of the β coefficient (odds ratio)
[f]95% confidence interval of exponentiation (β)

out determining the presence of ocular misalignment. The newly added schizophrenic samples in this study were also not screened for ocular misalignment. While the genetic contributions of *PHOX2B* Ala20 variations to general schizophrenia are more likely to be very weak or even negligible, even by considering genetic interactions with *ASCL1* (data not shown), these contributions may be evident only in a subset of schizophrenia (i.e., schizophrenia with strabismus). As might be expected according to this hypothesis, no association was apparent between *PHOX2B* and schizophrenia without strabismus ($P=0.076$) in our previous study (Toyota et al. 2004). We also tested here *ASCL1* as a singleton or *PHOX2B-ASCL1* epigenetic interaction (data not shown) for altered risk of another major psychosis, bipolar disorder, but no significant signals were detected. As a whole, the current results do not support these genetic mechanisms in the manifestation of functional psychoses.

PHOX2B/*ASCL1* and Parkinson's disease

PD is a common neurodegenerative disorder, characterized clinically by resting tremor, rigidity and bradykinesia. Neuropathological studies have revealed degeneration of the dopamine-producing substantia nigra and various other regions, including the basal ganglia, brainstem, autonomic nervous system and cerebral cortex (Dekker et al. 2003). Clinically defined PD represents an etiologically heterogeneous group of conditions encompassing a small population of individuals with Mendelian-type inheritance and a larger population of apparently sporadic cases (Hattori et al. 2003). Accumulating evidence has suggested that genetic predispositions exist even for sporadic PD (Marder et al. 1996). Dopamine deficiency is a primary pathomechanism in PD, and genes involved in dopamine neurotransmission, such as those for dopamine transporter, dopamine receptors, tyrosine hydroxylase, catechol-it O-methyltransferase and monoamine oxidase, have been examined in population-based association studies over the past decade. However, few of these genes have been definitively established as conferring susceptibility to sporadic PD (reviewed in Warner and Schapira 2003).

Perturbation of *PHOX2B* and *ASCL1* function has the potential to disturb catecholaminergic neurons, as these genes control the expression of the *TH* and *DBH* genes, which encode enzymes for the biosynthesis of dopamine (TH) and noradrenalin (TH and DBH) biosynthesis. Ludecke et al. (1996) reported a female infant who manifested L-dopa responsive Parkinsonism and carried a $Leu^{205}Pro$ mutation in exon 5 of the *TH* gene, reducing the catalytic ability of TH. The current study identified a positive association between PD and *ASCL1* polymorphisms. However, whether these *ASCL1* variants result in a predisposition to PD through direct effects on dopamine neurons remains unclear, as *ASCL1* expression in the human substantia nigra has not yet been confirmed. In contrast, expression of *ASCL1* in developing noradrenergic neurons in the human brainstem (locus coeruleus: LC) has been reported (De Pontual et al. 2003). The LC is known to play an important role in the pathophysiology of PD (reviewed in Gesi et al. 2000). Zarow et al. (2003) found more severe neuronal loss in the LC than in the substantia nigra in a postmortem examination of brains from PD patients. Mavridis et al. (1991) demonstrated that monkeys with LC lesions displayed impaired recovery from Parkinsonism induced using 1-methyl-4-phenyl-1,2,3,6-tetrahydropyridine (MPTP). Other studies have also shown that animals with LC lesions exhibit marked dopamine loss on administration of MPTP or methamphetamine (Bing et al. 1994; Fornai et al. 1997). These data suggest a protective role of the LC against the development of PD. Indeed, Srinivasan and Schmidt (2004) reported that the enhancement of noradrenergic transmission in the LC by β_2-adrenoceptor antagonists exerts a prophylactic effect against 6-hydroxydopamine-induced Parkinsonism. The present finding that the *ASCL1* allele containing 15 glutamines is less represented in PD than in controls might suggest that the 15-repeat allele could confer protective benefits compared to the most common 12-repeat allele, perhaps allowing the development of a well-functionalized LC that in turn helps to protect the substantia nigra from various insults.

Because of the presumed multigenic nature of complex traits, it would be desirable to analyze several polymorphisms jointly and investigate their effects and possible interactions on disease outcome (Ott 2001). One of the statistical methods that can be used to resolve this problem is logistic regression analysis. When applied to the current data, this analysis indicated that the dominant effect of *ASCL1* with the additive effect of *PHOX2B* was positive. The biological consequences resulting from the interaction between *ASCL1* and *PHOX2B* might thus offer useful insights into the pathogenesis of PD. Further studies elucidating the detailed mechanisms of this interaction are thus warranted.

Polyglutamine length variations in *ASCL1*

Polyglutamine expansion has been found in various neurodegenerative disorders, including Huntington's disease, spinocerebellar ataxia types 1, 2, 3 and 7, dentatorubral-pallido-luysian atrophy and spinobulbar muscular atrophy (Lipinski and Yuan 2004). The aggregation or accumulation of proteins with expanded polyglutamine sequences is considered to represent a critical contribution to neurodegeneration in these diseases. Generally these aggregate-forming proteins display more than 30 glutamine repeats, while *ASCL1* displays repeats of less than 20 glutamines. None of the Gln12 length variations for *ASCL1* detected in this study are thus likely to exert deteriorative effects on neurons. However, the functional consequences evoked by variations of the polyglutamine stretch in *ASCL1* are yet to be examined.

In summary, we performed an association study for *PHOX2B* and *ASCL1*, genes that are functionally closely related and display imperative roles in the development of neurons in the noradrenergic (dopaminergic) lineage, in three major neuropsychiatric diseases. Significant contributions of *ASCL1* and *ASCL1-PHOX2B* interactions to PD were detected. These results require genetic replication studies in different populations and further biological investigations to clarify the precise mechanisms and effects.

Acknowledgements This work was supported by RIKEN BSI Funds, Research on Brain Science Funds from the Ministry of Health Labor and Welfare, CREST funds from the Japan Science and Technology Agency and grants from the MEXT of Japan. We wish to thank Ms Ohba for technical assistance and the members of the Research Resource Center at the RIKEN Brain Science Institute for genotyping services.

References

American Psychiatric Association (1994) Diagnostic and statistical manual of mental disorders, 4th edn. American Psychiatric Association, Washington, D.C.

Bing G, Zhang Y, Watanabe Y, McEwen BS, Stone EA (1994) Locus coeruleus lesions potentiate neurotoxic effects of MPTP in dopaminergic neurons of the substantia nigra. Brain Res 668:261–265

Brownstein MJ, Carpten JD, Smith JR (1996) Modulation of non-templated nucleotide addition by Taq DNA polymerase: primer modifications that facilitate genotyping Biotechniques 20:1004–1006, 1008–1010

Cordell HJ, Clayton DG (2002) A unified stepwise regression procedure for evaluating the relative effects of polymorphisms within a gene using case/control or family data: application to HLA in type 1 diabetes. Am J Hum Genet 70:124–141

De Pontual L, Nepote V, Attie-Bitach T, Al Halabiah H, Trang H, Elghouzzi V, Levacher B, Benihoud K, Auge J, Faure C, Laudier B, Vekemans M, Munnich A, Perricaudet M, Guillemot F, Gaultier C, Lyonnet S, Simonneau M, Amiel J (2003) Noradrenergic neuronal development is impaired by mutation of the proneural *HASH-1* gene in congenital central hypoventilation syndrome (Ondine's curse). Hum Mol Genet 12:3173–3180

Dekker MC, Bonifati V, Van Duijn CM (2003) Parkinson's disease: piecing together a genetic jigsaw. Brain 126:1722–1733

Fornai F, Alessandri MG, Torracca MT, Bassi L, Corsini GU (1997) Effects of noradrenergic lesions on MPTP/MPP+ kinetics and MPTP-induced nigrostriatal dopamine depletions. J Pharmacol Exp Ther 283:100–107

Gesi M, Soldani P, Giorgi FS, Santinami A, Bonaccorsi I, Fornai F (2000) The role of the locus coeruleus in the development of Parkinson's disease. Neurosci Biobehav Rev 24:655–668

Hattori N, Kobayashi H, Sasaki-Hatano Y, Sato K, Mizuno Y (2003) Familial Parkinson's disease: a hint to elucidate the mechanisms of nigral degeneration. J Neurol 250(Suppl 3):III2–10

Itokawa M, Yamada K, Yoshitsugu K, Toyota T, Suga T, Ohba H, Watanabe A, Hattori E, Shimizu H, Kumakura T, Ebihara M, Meerabux JMA, Toru M, Yoshikawa T (2003) A microsatellite repeat in the promoter of the NMDA receptor 2A subunit (*GRIN2A*) gene suppresses transcriptional activity and correlates with chronic outcome in schizophrenia. Pharmacogenetics 13:271–278

Lipinski MM, Yuan J (2004) Mechanisms of cell death in polyglutamine expansion diseases. Curr Opin Pharmacol 4:85–90

Ludecke B, Knappskog PM, Clayton PT, Surtees RA, Clelland JD, Heales SJ, Brand MP, Bartholome K, Flatmark T (1996) Recessively inherited L-DOPA-responsive Parkinsonism in infancy caused by a point mutation (L205P) in the tyrosine hydroxylase gene. Hum Mol Genet 5:1023–1028

Marder K, Tang MX, Mejia H, Alfaro B, Cote L, Louis E, Groves J, Mayeux R (1996) Risk of Parkinson's disease among first-degree relatives: a community-based study. Neurology 47:155–160

Mavridis M, Degryse AD, Lategan AJ, Marien MR, Colpaert FC (1991) Effects of locus coeruleus lesions on parkinsonian signs, striatal dopamine and substantia nigra cell loss after 1-methyl-4-phenyl-1,2,3,6-tetrahydropyridine in monkeys: a possible role for the locus coeruleus in the progression of Parkinson's disease. Neuroscience 41:507–523

Ott J (2001) Neural networks and disease association studies. Am J Hum Genet 105:60–61

Pattyn A, Morin X, Cremer H, Goridis C, Brunet JF (1997) Expression and interactions of the two closely related homeobox genes *Phox2a* and *Phox2b* during neurogenesis. Development 124:4065–4075

Pattyn A, Morin X, Cremer H, Goridis C, Brunet JF (1999) The homeobox gene *Phox2b* is essential for the development of autonomic neural crest derivatives. Nature 399:366–370

Pattyn A, Goridis C, Brunet JF (2000) Specification of the central noradrenergic phenotype by the homeobox gene *Phox2b*. Mol Cell Neurosci 15:235–243

Renault B, Lieman J, Ward D, Krauter K, Kucherlapati R (1995) Localization of the human achaete-scute homolog gene (*ASCL1*) distal to phenylalanine hydroxylase (*PAH*) and proximal to tumor rejection antigen (*TRA1*) on chromosome 12q22-q23. Genomics 30:81–83

Schneider RD, Excofier L (2000) Arlequin: a software for population genetics data analysis, 2 edn, version 2.000. Genetics and Biometry Laboratory, Department of Anthropology, University of Geneva

Sham PC, Curtis D (1995) Monte Carlo tests for associations between disease and alleles at highly polymorphic loci. Ann Hum Genet 59:97–105

Srinivasan J, Schmidt WJ (2004) Treatment with alpha2-adrenoceptor antagonist, 2-methoxy idazoxan, protects 6-hydroxydopamine-induced Parkinsonian symptoms in rats: neurochemical and behavioral evidence. Behav Brain Res 154:353–363

Sriuranpong V, Borges MW, Strock CL, Nakakura EK, Watkins DN, Blaumueller CM, Nelkin BD, Ball DW (2002) Notch signaling induces rapid degradation of achaete-scute homolog 1. Mol Cell Biol 22:3129–3139